Articles in PresS. J Neurophysiol (January 18, 2017). doi:10.1152/jn.00911.2016

A Neural Locus for Spatial-Frequency Specific Saccadic Suppression in Visual-Motor Neurons of the Primate Superior Colliculus

Chih-Yang Chen[1,2] and Ziad M. Hafed[1]

1. Werner Reichardt Centre for Integrative Neuroscience, Tuebingen University, Tuebingen, BW, 72076, Germany
2. Graduate School of Neural and Behavioural Sciences, International Max Planck Research School, Tuebingen University, Tuebingen, BW, 72074, Germany

Abbreviated Title:

Saccadic suppression in monkey superior colliculus

Corresponding Author:
Ziad M. Hafed
Werner Reichardt Centre for Integrative Neuroscience
Otfried-Mueller Str. 25
Tuebingen, BW, 72076, Germany
Tel: +49 7071 29-88819
E-mail: ziad.m.hafed@cin.uni-tuebingen.de

Abstract

Saccades cause rapid retinal-image shifts that go perceptually unnoticed several times per second. The mechanisms for saccadic suppression have been controversial, in part due to sparse understanding of neural substrates. Here we uncovered an unexpectedly specific neural locus for spatial-frequency specific saccadic suppression in the superior colliculus (SC). We first developed a sensitive behavioral measure of suppression in two macaque monkeys, demonstrating selectivity to low spatial frequencies similar to that observed in earlier behavioral studies. We then investigated visual responses in either purely visual SC neurons or anatomically-deeper visual-motor neurons, which are also involved in saccade generation commands. Surprisingly, visual-motor neurons showed the strongest visual suppression, and the suppression was dependent on spatial frequency like in behavior. Most importantly, suppression selectivity for spatial frequency in visual-motor neurons was highly predictive of behavioral suppression effects in each individual animal, with our recorded population explaining up to ~74% of behavioral variance even on completely different experimental sessions. Visual SC neurons had mild suppression, which was unselective for spatial frequency and thus only explaining up to ~48% of behavioral variance. In terms of spatial-frequency specific saccadic suppression, our results run contrary to predictions that may be associated with a hypothesized SC saccadic suppression mechanism, in which a motor command in the visual-motor and motor neurons is first relayed to the more superficial purely visual neurons to suppress them, and to then potentially be fed back to cortex. Instead, an extra-retinal modulatory signal mediating spatial-frequency specific suppression may already be established in visual-motor neurons.

New & Noteworthy

Saccades, which repeatedly re-align the line of sight, introduce spurious signals in retinal images that normally go unnoticed. In part, this happens because of peri-saccadic suppression of visual sensitivity, which is known to depend on spatial frequency. Here we discovered that a specific sub-type of superior colliculus (SC) neurons demonstrates spatial-frequency dependent suppression. Curiously, it is the neurons that help mediate the saccadic command itself that exhibit such suppression, and not the purely visual ones.

Keywords

Saccades; Microsaccades; Superior colliculus; Saccadic suppression; Perceptual stability

Introduction

A long standing question in visual neuroscience has been on how we normally experience a sense of perceptual stability despite incessant eye movements (Wurtz 2008). Saccadic eye movements, in particular, dramatically alter retinal images several times per second. During each saccade, retinal images undergo rapid motion, which can be beyond the range of motion sensitivity of many neurons. Such motion ought, at least in principle, to cause a brief period of "grey out" every time a saccade occurs (Campbell and Wurtz 1978; Matin 1974; Wurtz 2008; Wurtz et al. 2011), much like the grey out experienced while standing near train tracks and high-speed trains sweep by.

Several theories on why we do not experience saccade-related visual disruptions have been debated in the literature. On the one hand, purely visual mechanisms, such as masking (Matin et al. 1972), can be sufficient to suppress perception of saccade-induced grey out and/or motion (Wurtz 2008). Consistent with this, people are not entirely "blind" during saccades, as long as spatio-temporal properties of peri-saccadic stimuli remain within sensitivity ranges of visual neurons (Burr and Ross 1982; Castet et al. 2001; Castet and Masson 2000; Garcia-Perez and Peli 2011; Ilg and Hoffmann 1993; Matin et al. 1972; Ross et al. 1996). On the other hand, extra-retinal mechanisms (Sperry 1950; von Holst and Mittelstaedt 1950) for suppression are supported by the lack of suppression during simulated image displacements (Diamond et al. 2000), the dependence of suppression on spatial frequency (Burr et al. 1982; Burr et al. 1994; Hass and Horwitz

84 2011; Volkmann et al. 1978), and the observation of saccade-related modulation of neural
85 excitability in the absence of visual stimulation (Rajkai et al. 2008).
86
87 While it is likely that a combination of visual and extra-retinal mechanisms co-exist
88 (Wurtz 2008), further understanding of neural mechanisms is needed to resolve some of
89 the debates surrounding saccadic suppression. We were particularly interested in
90 potential mechanisms for extra-retinal suppression, whose sources remain elusive. For
91 example, it was suggested from behavioral studies that selective suppression of low
92 spatial frequencies is evidence for selective magno-cellular (achromatic) pathway
93 suppression (Burr et al. 1994). However, in lateral geniculate nucleus (LGN) and primary
94 visual cortex (V1), two early visual areas possessing clear magno- and parvo-cellular
95 segregations, selective magno-cellular suppression is not established (Hass and Horwitz
96 2011; Kleiser et al. 2004; Ramcharan et al. 2001; Reppas et al. 2002; Royal et al. 2006).
97 In addition, a hypothesis about a source of saccadic suppression is that a "corollary" of
98 saccade commands in visual-motor and motor neurons of the superior colliculus (SC) is
99 fed back to superficial purely visual neurons to suppress their sensitivity, and to jumpstart
100 a putative feedback pathway for cortical suppression through pulvinar (Berman and
101 Wurtz 2008; 2010; 2011; Isa and Hall 2009; Lee et al. 2007; Phongphanphanee et al.
102 2011; Wurtz 2008; Wurtz et al. 2011). However, evidence for an SC saccadic suppression
103 pathway from visual-motor/motor neurons to visual neurons comes primarily from rodent
104 SC slices (Isa and Hall 2009; Lee et al. 2007; Phongphanphanee et al. 2011). In the
105 awake, behaving primate, findings of stronger suppression in visual-motor rather than
106 visual neurons (Chen et al. 2015; Hafed et al. 2015; Hafed and Krauzlis 2010) suggest a

107 more nuanced set of mechanisms. Moreover, spatial-frequency specific suppression of
108 visual sensitivity in either visual or visual-motor SC neurons has not yet been
109 investigated.
110
111 In this study, we visited the question of neural loci for saccadic suppression in the SC by
112 looking for spatial-frequency specificity of visual suppression. We have previously
113 shown that SC neurons exhibit time courses of saccadic suppression remarkably similar
114 to those of perceptual effects in humans (Hafed and Krauzlis 2010). However, our
115 previous experiments did not investigate any potential spatial-frequency dependence in
116 saccadic suppression, as might be expected from earlier human experiments (Burr et al.
117 1994). Our earlier experiments only presented a white bar stimulus within a neuron's
118 visual response field (RF). Thus, here, we adapted our behavioral paradigm from (Hafed
119 and Krauzlis 2010) to first establish *selectivity* in saccadic suppression during this
120 paradigm, and we then asked whether *visual* neural modulations in either purely visual or
121 visual-motor SC neurons would reflect such selectivity. Contrary to what we might have
122 predicted based on a suppressive pathway from deep to superficial layers (Isa and Hall
123 2009; Lee et al. 2007; Phongphanphanee et al. 2011), we observed spatial-frequency
124 specific saccadic suppression only in the deeper visual-motor neurons. Visual neurons
125 showed mild suppression, but this suppression was not modulated as a function of spatial
126 frequency. Moreover, we recorded local field potentials (LFP's), as a proxy for
127 population and synaptic activity around our isolated neurons (Hafed and Chen 2016;
128 Iketa et al. 2015), and we found evidence that the visual suppression of firing rates that
129 we observed in isolated neurons may have been mediated by the presence of modulatory

130 signals in the SC associated with the motor generation of saccades, and particularly in the
131 visual-motor layers. Our results suggest that the SC may indeed be relevant for spatial-
132 frequency specific saccadic suppression, which has been reported previously in humans
133 (Burr et al. 1994), but that the putatively extra-retinal modulatory signal mediating
134 suppression may already be established in the visual-motor neurons.
135
136 From a technical standpoint, we exploited microsaccades to study saccadic suppression in
137 this study because microsaccades offer important experimental advantages while at the
138 same time being mechanistically similar to larger saccades (Hafed 2011; Hafed et al.
139 2015; Hafed et al. 2009; Zuber et al. 1965). First, microsaccades are small (median
140 amplitude in our data: ~7.5 min arc). Thus, pre- and post-movement visual RF's are not
141 displaced by much, minimizing the problem of dramatic spatial image shifts caused by
142 saccades (Wurtz 2008; Wurtz et al. 2011). Experimentally, this meant presenting the
143 same stimulus at the same screen location with and without microsaccades to isolate
144 suppression effects. Second, microsaccades have velocities significantly <100 deg/s
145 (median peak velocity in our data: ~17.7 deg/s). Thus, image motion caused by
146 microsaccades is well within the range of motion sensitivity, even for small features
147 (Thiele et al. 2002), allowing us to study suppression even when no motion-induced grey
148 out is expected to occur. Third, we have previously shown, with simple white bars, that
149 SC visual sensitivity exhibits pre-, peri-, and post-microsaccadic suppression that is
150 similar in time course and amplitude to perceptual saccadic suppression in humans with
151 larger saccades, and we have also demonstrated a sensitive behavioral paradigm for the
152 same phenomenon (Hafed and Krauzlis 2010). Fourth, and more importantly, we avoided

potential masking effects by only presenting stimuli immediately *after* microsaccades. This allowed us to study suppression after saccades, which is known to still occur (Chen et al. 2015; Hafed and Krauzlis 2010; Zuber et al. 1966), and to ensure comparing "no-microsaccade" to "microsaccade" conditions without the latter involving saccade-induced retinal image motion. Finally, it was already established a long time ago that at the behavioral level, microsaccades are associated with similar suppression to larger saccades (Zuber et al. 1966), and that saccadic suppression is also expected to occur far away from the movement endpoint (Knoll et al. 2011); this meant that using microsaccades as a model system for saccadic suppression was reasonable. Thus, the logic of all of our experiments was to present high-contrast gratings (80% contrast), which were highly visible and well within the saturation regime of SC contrast sensitivity curves (Chen et al. 2015; Hafed and Chen 2016; Li and Basso 2008), and to ask whether either behavioral or visual neural responses to these gratings were altered if the gratings appeared immediately after a microsaccade.

Materials and Methods

Animal Preparation

Ethics committees at regional governmental offices in Tuebingen approved experiments. Monkeys N and P (male, *Macaca mulatta*, aged 7 years) were prepared as detailed earlier (Chen and Hafed 2013; Chen et al. 2015; Hafed and Chen 2016; Hafed and Ignashchenkova 2013). Briefly, under isoflurane anesthesia and aseptic conditions, we first attached a head-holder to the skull. The head-holder consisted of a titanium implant that was embedded under the skin and attached to the skull using titanium screws. In a subsequent surgery, we made a small skin incision on top of the head and attached a metal connector to the previously implanted head-holder. This connector acted as the interface for fixing the head to a standard position in the lab during data collection. In the same surgery, a scleral search coil was implanted in one eye to allow measuring eye movements with high temporal and spatial precision using the magnetic induction technique (Fuchs and Robinson 1966; Judge et al. 1980). After the animals completed the behavioral training and experimental sessions, we implanted recording chambers to access the SC. The chambers were placed on the midline, aimed at 1 mm posterior of and 15 mm above the inter-aural line. Chambers were tilted posterior of vertical (by 35 and 38 deg for N and P, respectively).

Behavioral Tasks

In all tasks, monkeys initially fixated a small, white spot presented over a gray background (Chen and Hafed 2013; Chen et al. 2015; Hafed and Ignashchenkova 2013). Spot and background luminance were 72 and 21 Cd/m^2, respectively.

Behavioral tests. Trials started with an initial fixation interval of random duration (between 600 and 1500 ms). After this interval, we initiated a real-time process to detect microsaccades (Chen and Hafed 2013). Briefly, this process evaluated instantaneous radial eye velocity based on recently sampled eye positions, and it flagged the presence of a microsaccade when this velocity exceeded a user-defined threshold. If a microsaccade was detected within 500 ms, a stationary vertical Gabor grating (having 80% contrast relative to background luminance) appeared at 3.5 deg to the right or left of fixation, and the fixation spot was removed simultaneously. Monkeys oriented to the grating using a saccadic eye movement, and saccadic reaction time (RT) served as a sensitive behavioral measure of SC visual response strength (Boehnke and Munoz 2008; Hafed and Chen 2016; Hafed et al. 2015; Hafed and Krauzlis 2010; Tian et al. 2016; also see Discussion). Because of their extensive training on visually-guided saccades, our monkeys were likely making speeded reactions to the gratings, further justifying the use of RT. Grating onset occurred ~25, 50, 75, 100, 150, or 200 ms after online microsaccade detection, and we later measured precise times of microsaccade onset during data analysis for all results presented in this paper (see Data Analysis below). Our choice of times to sample above was based on earlier observations that saccadic suppression effects in the SC subside by ~100 ms after the movements (Chen et al. 2015; Hafed and Krauzlis

2010). If no microsaccade was detected during our 500 ms online detection window, a grating was presented anyway, and the data contributed to "baseline" measurements (i.e. ones with the stimulus appearing without any nearby microsaccades). The grating was 2 deg in diameter. Spatial frequency in cycles per degree (cpd) was one of five values: 0.56, 1.11, 2.22, 4.44, 11.11 (Hafed and Chen 2016), and phase was randomized. Our monitor resolution allowed displaying the highest spatial frequency without aliasing and distortion. We collected 8153 and 7117 trials from monkeys N and P, respectively. We removed trials with an intervening microsaccade between fixation spot removal and the orienting saccade.

Neural recordings. We isolated single neurons online, and we identified their RF locations and sizes using standard saccade tasks (Chen et al. 2015; Hafed and Chen 2016). We then ran our main experimental paradigm. In each trial, monkeys fixated while we presented a similar vertical grating to the one we used in behavioral tests above (i.e. with similar contrast and spatial frequency ranges), but the grating was now inside the recorded neuron's RF. Grating size was optimized for the recorded neuron, and was specifically chosen to fill as much of the RF as possible (and showing >1 cycle of the lowest spatial frequency). Task timing was identical to that in (Chen et al. 2015); briefly, a grating was presented for 250 ms while monkeys fixated, and the monkeys never generated any saccadic or manual responses to the grating (they simply maintained fixation, during which they generated microsaccades, and they were rewarded at the end of the 250 ms stimulus presentation phase for maintaining fixation). We collected data from 90 neurons (n=39 from monkey N and n=51 from monkey P), covering 1-24 deg

eccentricities. We classified neurons as purely visual neurons or visual-motor neurons using previous criteria from visually-guided and memory-guided saccade tasks (Chen et al. 2015; Hafed and Chen 2016). To ensure sufficient microsaccades for statistical analyses (i.e. with sufficient trials having stimulus onset within the critical post-movement intervals that we analyzed), we collected >800 trials per neuron. We then separated trials as ones having no microsaccades within +/- 100 ms from grating onset (>100 trials per neuron; mean: 289 trials per neuron; median: 191 trials per neuron) or ones with grating onset within 50 ms *after* microsaccades (>25 trials per neuron; mean: 79 trials per neuron; median: 79 trials per neuron). The former trials provided an estimate of "baseline" responses without the influence of saccadic suppression, and the latter trials provided an estimate of the suppressed responses due to saccadic suppression. Moreover, the times chosen were justified based on previous descriptions of the time courses of saccadic suppression (e.g. Hafed and Krauzlis 2010; Zuber et al. 1966). Some of our analyses also included grating onsets up to 100 ms after microsaccades.

It is important to note here that for all neurons reported in this paper, we never observed a microsaccade-related movement burst (Hafed et al. 2009; Hafed and Krauzlis 2012). Thus, even for stimuli appearing immediately after a microsaccade, the neural responses that we analyzed were *visual* bursts in response to stimulus onset, and not movement-related saccade or microsaccade bursts. The only difference between purely visual and visual-motor neurons in this study was that visual-motor neurons would, in principle, exhibit a saccade-related burst if the monkeys were to hypothetically generate saccades towards the RF location (but not if they generated smaller microsaccades during

fixation). Thus, any neural modulations that we report in this study are not direct microsaccade-related motor bursts.

It is also important to note that our monkeys did not generate any targeting saccades to the gratings during recordings. We were simply studying *visual* sensitivity if a stimulus appeared near an eye movement. Our approach was thus very similar to classic ways of studying neural correlates of saccadic suppression (i.e. monkeys make saccades while neurons are visually stimulated; e.g. Zanos et al. 2016; Hafed and Krauzlis 2010; Bremmer et al. 2009).

Data Analysis

In all figures, we plotted mean values (along with suitable measures of variance, like s.e.m.) for the parameters that we were visualizing; we used mean in the figures because this is a standard way of presenting data. However, in quantitative descriptions in the text, we sometimes reported median values in addition to mean values, and for statistical analyses, we always performed non-parametric statistical tests because our neural and behavioral data were not always normally distributed.

In all neural data analyses, we combined results from both monkeys. This was justified because the two monkeys showed consistent results with each other, and also consistent results with the prior literature (e.g. Hafed and Krauzlis 2010; Chen et al. 2015). However, for relating neural activity to behavior, it was unfair to compare the behavior of an individual monkey to neural data combined from both animals. Thus, only when

283 relating neural activity to behavior, we separated the neural data into individual monkey
284 data. This had the added advantage of demonstrating the consistency of neural results
285 across individual monkeys, justifying our pooling of the animals for the summary figures
286 of neural data analyses.
287
288 *Behavioral analyses.* For behavior, we measured RT as a function of spatial frequency
289 and time of grating onset relative to microsaccades. We also counted "express saccade"
290 RT trials, which we defined as trials with RT <100 ms (Fischer and Boch 1983).
291
292 During offline analysis, we re-detected microsaccades using previously described
293 methods (Hafed et al. 2009), because we could now use non-causal filters for better
294 estimates of eye velocity, and because we could also refine the time of movement
295 onset/end based on eye acceleration. We used such detection to identify grating onset
296 time relative to microsaccade onset or offset. We defined no microsaccade trials as trials
297 with no microsaccades <250 ms from grating onset. RT on these trials constituted our
298 baseline.
299
300 *Firing rate analyses.* For neural data, we measured stimulus-evoked firing rate after the
301 onset of a given spatial-frequency grating under two scenarios: (1) when the grating
302 appeared without any nearby microsaccades within +/- 100 ms, and (2) when the grating
303 appeared immediately after a microsaccade. Baseline, no-microsaccade spatial frequency
304 tuning curves (i.e. responses for each given spatial frequency) were described recently
305 (Hafed and Chen 2016), but here we analyzed microsaccadic influences on these curves.

306 We did not analyze trials with grating onset immediately before or during microsaccades,
307 to avoid pre-movement modulations (Chen et al. 2015; Hafed 2013) and retinal-image
308 shift effects caused by movement of the eyes, but previous studies have demonstrated
309 suppression also during these intervals (Hafed and Krauzlis 2010).
310
311 To analyze stimulus-evoked firing rate, we measured peak visual response 20-150 ms
312 after grating onset. To compare visual sensitivity on microsaccade and no-microsaccade
313 trials, we created a "normalized firing rate" modulation index for each individual spatial
314 frequency. We measured firing rate on microsaccade trials (i.e. trials with grating onset
315 within 50 ms after microsaccades) and divided it by rate on no-microsaccade trials (i.e.
316 trials with no microsaccades within <100 ms from grating onset). A value <1 indicates
317 suppression. Note that we only considered neurons with >5 spikes/s stimulus-evoked
318 response (even on 11.11 cpd trials, which frequently had the lowest firing rates), thus
319 avoiding "divide by zero" problems. Also, note that this modulation index isolates
320 changes in visual sensitivity associated with saccadic suppression, regardless of how
321 visual sensitivity itself might depend on spatial frequency without microsaccades. For
322 example, visual responses in general are expected to be weaker for high spatial
323 frequencies (Hafed and Chen 2016); however, our modulation index would normalize
324 activity within a given spatial frequency in order to isolate any further suppression of
325 visual sensitivity due to saccadic suppression.
326
327 In our analyses (including behavioral analyses), we combined microsaccades towards or
328 away from the grating because suppression is not direction-dependent in the post-

movement interval that we focused on (Chen et al. 2015). However, we also confirmed this when analyzing the present data set (e.g. see Fig. 5). Our population analyses also combined neurons representing different eccentricities. We did so because we found that suppression is independent of eccentricity during the post-movement interval that we focused on (Chen et al. 2015).

To investigate the relationship between neural modulations and behavioral effects, we correlated behavioral patterns of saccadic suppression from the behavioral tests to neural modulations obtained from the recordings. For example, we related visual response firing rate strength to mean RT as a function of time of grating onset after microsaccades. The mean RT was obtained from all collected behavioral trials (i.e. including the minority of express RT trials; see Results) because visual responses are expected to affect overall behavior, without being specifically "labeled" in the brain as belonging to either a potential express RT trial or a regular trial.

For all analyses with time courses, we used bin steps of 10 ms and bin widths of 50 ms (except for Fig. 2G, H, J, K with both bin steps and bin widths of 25 ms).

Local field potential (LFP) analyses. To analyze LFP's, we sampled neurophysiological activity at 40 KHz. The signal was first filtered in hardware (0.7-6 KHz). We then removed 50, 100, and 150 Hz line noise using an IIR notch filter and then applied a zero-phase-lag lowpass filter (300 Hz cutoff). We finally down-sampled to 1 KHz. We analyzed filtered LFP traces like firing rates (Hafed and Chen 2016; Ikeda et al. 2015),

and we classified electrode track locations as visual or visual-motor according to the neurons isolated from these tracks in the same sessions (Hafed and Chen 2016).

To obtain a measure of intrinsic peri-microsaccadic modulation of LFP's independent of visual stimulation, we took all microsaccades occurring in a pre-stimulus interval (20-100 ms before grating onset). We then aligned LFP traces on either microsaccade onset or end, in order to uncover any systematic LFP modulation time-locked to the movement execution. To compare this data to a baseline, we took identically-long analysis intervals, again from pre-stimulus periods, but with no microsaccades occurring anywhere within these intervals.

To correlate LFP responses to behavioral dynamics of saccadic suppression (similar to what we did with firing rates), we measured peak transient LFP deflection as the minimum in the stimulus-evoked LFP trace 20-150 ms after grating onset. We created a "field potential index" by dividing this measurement on microsaccade trials by that on no-microsaccade trials. An index >1 indicates enhancement. For a control analysis, we computed the index after correcting for a microsaccade-related LFP level shift that may have happened due to intrinsic peri-microsaccadic modulation of the LFP independent of visual stimulation. We did this according to the following procedure. On microsaccade trials, we measured the average LFP value -25 to 25 ms from grating onset. We then subtracted the peak stimulus-evoked LFP deflection from this baseline measurement before dividing by the no-microsaccade trials. If an intrinsic peri-microsaccadic LFP

modulation explained our results of LFP enhancement with increasing spatial frequency (see Results), then the baseline-shifted index should show no enhancement.

We also analyzed transient stimulus-evoked LFP deflection latency. We found the first time at which the LFP was >2 s.d. away from baseline LFP (calculated as the mean LFP value -25 to 25 ms from grating onset), and there also had to be >5 ms of continuous >2 s.d. deviation from baseline. We did this separately for microsaccade and no-microsaccade trials, and we subtracted the measurements to obtain the influences of saccadic suppression on stimulus-evoked LFP deflection latency. If the LFP transient deflection occurs faster on microsaccade trials, then the subtraction gives a negative value.

Results

Selective Microsaccadic Suppression of Low Spatial Frequencies in Behavior

Isolation of spatial-frequency specific saccadic suppression requires demonstrating a selective form of suppression in behavior, and subsequently asking which neurons reflect such selectivity. We thus first developed a behavioral measure demonstrating selective suppression, which was based on our earlier results (Hafed and Krauzlis 2010). We did so for microsaccades because they are mechanistically similar to larger saccades, while at the same time providing important experimental advantages (see Introduction). Monkeys fixated, and we initiated a computer process for real-time microsaccade detection (Chen and Hafed 2013). After such detection by a programmable delay, we presented a stationary vertical Gabor grating (80% contrast). The monkeys oriented towards the grating as fast as possible. Because SC *visual* bursts are strongly correlated with RT (Boehnke and Munoz 2008; Chen et al. 2015; Hafed and Chen 2016; Hafed et al. 2015; Hafed and Krauzlis 2010; Tian et al. 2016), we used RT changes in this task as a sensitive measure of microsaccadic influences on visual sensitivity (Hafed and Krauzlis 2010; Tian et al. 2016; also see Discussion).

Similar to previously reported perceptual effects with large saccades (Burr et al. 1994) and also microsaccades (Hass and Horwitz 2011), grating onset after microsaccades had a strong, yet selective, impact on behavior in our monkeys. Figure 1A shows example eye position (left) and velocity (right) traces from one monkey while we presented a 1.11 cpd grating. The black traces show trials without microsaccades <250 ms from grating onset,

and the gray traces show trials with grating onset ~20-100 ms after microsaccades. There was a marked increase in RT during microsaccade trials (Fig. 1A). However, when we presented, say, 4.44 cpd (Fig. 1B) or 11.11 cpd (Fig. 1C) gratings, RT's on microsaccade and no-microsaccade trials were more similar to each other (compare the gray and black distributions in each panel). Thus, the microsaccadic suppressive effect (causing slower RT's relative to no-microsaccade baselines) was diminished for higher-frequency gratings. These sample-trial results demonstrate a correlate in our monkeys of selective perceptual suppression of low spatial frequencies by large saccades and also microsaccades (Burr et al. 1982; Burr et al. 1994; Hass and Horwitz 2011; Volkmann et al. 1978), even though we used a different behavioral measure.

Across behavioral sessions, both monkeys showed selective RT increases for low spatial frequencies (Fig. 2A, D). On no-microsaccade trials (black curves), mean RT increased with increasing spatial frequency, as expected from dynamics of the early visual system (Breitmeyer 1975) and SC (unpublished observations). For example, mean RT for 0.56 cpd gratings was 109.1 ms +/- 1.37 ms s.e.m. in monkey N and 179.8 ms +/- 2.12 ms s.e.m. in monkey P, whereas it was 178.4 ms +/- 4.37 ms s.e.m. in monkey N and 224.5 ms +/- 4.2 ms s.e.m. in monkey P for 11.11 cpd. This effect was statistically significant ($p<0.01$ for monkey N and $p<0.01$ for monkey P, Kruskal-Wallis test with spatial frequency as the main factor). However, with gratings appearing ~20-100 ms after microsaccades, the RT cost relative to no-microsaccade trials (i.e. the *difference* in RT between microsaccade and no-microsaccade trials) was strongest for the lowest spatial frequencies (Fig. 2B, E; $p<0.01$ for monkey N and $p<0.01$ for monkey P, Kruskal-Wallis

433 test with spatial frequency as the main factor). This effect was not a ceiling effect on RT
434 because it was still possible for RT to increase even more at higher spatial frequencies.
435 For example, at 4.44 cpd, RT on microsaccade and no-microsaccade trials was similar
436 (Fig. 2A, D; magenta rectangles), but it got even slower for 11.11 cpd regardless of eye
437 movements. This effect is also seen in the raw black traces of Fig. 1C, exhibiting longer
438 RT values than the black traces of Fig. 1B. Importantly, even at 11.11 cpd, RT on
439 microsaccade trials was modestly longer than on no-microsaccade trials in both animals
440 (Fig. 2A, D), suggesting that the impact of microsaccades could still be visible even when
441 RT itself was very long because of high spatial frequencies. Thus, the reduction in RT
442 differences between microsaccade and no-microsaccade trials for high spatial frequencies
443 (Fig. 2B, E) was suggestive of a selective suppression of low spatial frequencies, and not
444 necessarily a ceiling effect on RT.
445
446 On a small subset of the trials in Fig. 2A, D, our monkeys' RT values fell within a so-
447 called "express" range (which we defined as trials having RT <100 ms). Overall, 11.05%
448 and 6.34% of all trials in monkeys N and P, respectively, were express. These trials
449 formed a small, but distinct peak in RT distributions typical of express saccades
450 (although this small peak appeared to merge with regular RT distributions for the lowest
451 spatial frequency in monkey N because of this monkey's low overall RT values). We thus
452 additionally analyzed how these specific express responses were affected by
453 microsaccades occurring near grating onset. In both monkeys (Fig. 2C, F), there was a
454 reduction in express RT trials (i.e. the small low-latency peak in RT distributions was
455 further reduced); moreover, the change in express RT trial likelihood between

456 microsaccade and no-microsaccade trials was largest for low spatial frequencies,
457 consistent with the spatial-frequency specific lengthening of RT's in Fig. 2A, D, B, E.
458 Thus, the spatial-frequency specific microsaccadic influence that we describe in this
459 study affected our monkeys' behavior even when analyzing express RT trials.
460
461 Our behavioral paradigm also provided rich information about saccadic suppression
462 dynamics, which we could later use to relate to SC neural modulations. For example, we
463 evaluated microsaccadic suppression time courses across different spatial frequencies.
464 Figures 2G, H, J, K illustrate this by plotting mean RT from Fig. 2A, D as a function of
465 when a 1.11 or 4.44 cpd grating appeared after microsaccades. Microsaccadic occurrence
466 had a clear time course of RT costs for each spatial frequency, with both monkeys
467 showing lower RT costs for the higher spatial frequency immediately after
468 microsaccades, and then a gradual return towards the baseline no-microsaccade
469 performance for a given frequency. Similarly, when we only focused on the subset of
470 express RT trials, we found that the likelihood of express RT's was decreased
471 immediately after microsaccades and gradually recovered (i.e. increased), and the
472 magnitude of the recovery was again spatial-frequency specific (Fig. 2I, L).
473
474 Therefore, using a behavioral measure sensitive to SC visual response strength (Boehnke
475 and Munoz 2008; Hafed and Chen 2016; Hafed et al. 2015; Hafed and Krauzlis 2010),
476 we found a robust and selective pattern of microsaccadic suppression, which we think is
477 analogous to perceptual suppression in humans with large saccades (Burr et al. 1982;
478 Burr et al. 1994; Volkmann et al. 1978). Note that our results are also consistent with

spatial-frequency specific suppression of contrast detection performance in monkeys around the time of microsaccades (Hass and Horwitz 2011), which confirms that microsaccades have similar effects to larger saccades, and that our RT measures in the present study were indeed sufficient to establish a behavioral effect in our animals. We were now in a position to evaluate neural correlates of this behavioral effect, and to specifically test whether spatial-frequency specific suppression would emerge in purely visual SC neurons, as we might predict from a previously published hypothesis about an SC circuit model for saccadic suppression (Berman and Wurtz 2008; 2010; 2011; Isa and Hall 2009; Lee et al. 2007; Phongphanphanee et al. 2011; Wurtz 2008; Wurtz et al. 2011).

Selective Suppression of Low Spatial Frequencies in Visual-Motor but not Visual SC Neurons

Using the same animals but in completely different experimental sessions not requiring any saccadic responses at all (Materials and Methods), we recorded the activity of purely visual SC neurons (24 neurons; located 680 +/- 95 s.e.m. μm below SC surface) or visual-motor neurons (66 neurons; 1159 +/- 66 s.e.m. μm below SC surface). Both types of neurons exhibit robust *visual* responses, but the question remains as to which would show spatial-frequency specific suppression. We presented gratings similar to those used in Figs. 1-2 inside each neuron's RF (Materials and Methods). However, the task was now a fixation task with no saccadic eye movements towards the gratings; we only analyzed either no-microsaccade trials or trials in which the gratings appeared immediately *after* microsaccades (Materials and Methods).

Ensuring fixation during the recordings was especially important to demonstrate behavioral relevance of our neural modulations. Specifically, one of our goals was to directly correlate neural dynamics to behavior in each animal (as will be presented later). Showing that a specific SC cell class is highly correlated with behavior compared to another cell class, *even* when the correlations are made across completely independent sessions and tasks, would demonstrate the behavioral relevance of the cell class. Moreover, demonstrating that neural suppression dynamics appear on *visual* responses, even in the complete absence of an overt response, shows that it is *sensory* responses that matter during saccadic suppression. Finally, ensuring fixation avoided influences on visual sensitivity that take place during tasks requiring monkeys to generate a subsequent saccade to the presented stimulus (Li and Basso 2008).

Visual-motor SC neurons showed the strongest saccadic suppression, and in a spatial-frequency selective manner. Figure 3A shows the activity of two sample pure visual neurons (one per row) during presentations of different spatial frequencies (across columns), and Fig. 3B shows the activity of two sample visual-motor neurons (in the same format). In each panel, saturated colors show activity with no microsaccades <100 ms from grating onset, and unsaturated colors show activity when the same grating was presented within 50 ms after microsaccades. In no-microsaccade trials, all neurons showed expected visual bursts, but burst strength varied with spatial frequency (Fig. 3, saturated colors). This is suggestive of spatial-frequency tuning (Hafed and Chen 2016), but our purpose here was to investigate suppression relative to no-microsaccade

525 responses; thus, we scaled the y-axis in each panel such that across panels, no-
526 microsaccade curves visually appeared to be roughly equal in height. Using such scaling,
527 visual-burst suppression (unsaturated colors) was rendered clearer (quantitatively, we
528 always measured suppression relative to the no-microsaccade responses *within* each
529 given spatial frequency independently and not across spatial frequencies; Materials and
530 Methods). Importantly, there were differences in suppression patterns between visual and
531 visual-motor neurons. For the visual neurons (Fig. 3A), suppression was mild and
532 relatively inconsistent across spatial frequencies; for the visual-motor neurons (Fig. 3B),
533 there was strong suppression for the lowest spatial frequency (Neuron #3: ~32%; Neuron
534 #4: ~38%; $p<0.01$ for each neuron, Wilcoxon rank sum test), and there was also a
535 systematic reduction in suppression strength with increasing frequency (by 4.44 and
536 11.11 cpd, there was no suppression left; $p=0.49$ for 4.44 cpd and $p=0.41$ for 11.11 cpd in
537 Neuron #3, and $p=0.15$ for 4.44 cpd and $p=0.99$ for 11.11 cpd in Neuron #4, Wilcoxon
538 rank sum test). Importantly, the eye movement associated with suppression in all panels
539 had ended before grating onset. Thus, the suppression cannot be attributed to blurring of
540 the gratings by eye movements.
541
542 Across neurons, there was selective suppression of visual sensitivity as a function of
543 spatial frequency, but only in visual-motor neurons. Figure 4A summarizes these findings
544 by plotting a suppression index (Materials and Methods) as a function of spatial
545 frequency. Peak visual response was suppressed in both visual and visual-motor neurons
546 (suppression index <1). However, the suppression was not spatial-frequency selective,
547 and it was weaker, in visual neurons; in visual-motor neurons, there was strong

548 suppression for the lowest spatial frequencies, and the effect gradually dissipated away
549 with increasing frequency. Quantitatively, the average suppression value in visual
550 neurons was 11% across spatial frequencies, and it was 22% in visual-motor neurons.
551 When separating low and high spatial frequencies, the average suppression value in
552 visual neurons for the lowest two spatial frequencies or the highest two spatial
553 frequencies was 11%, meaning that the suppression value was similar for the two groups
554 of frequencies ($p=0.77$, Wilcoxon rank sum test). On the other hand, visual-motor
555 neurons were suppressed by 23% for the lowest two spatial frequencies and 17% for the
556 highest two spatial frequencies, and the difference between the groups of spatial
557 frequencies was significant ($p<0.01$, Wilcoxon rank sum test).
558
559 A difference between visual and visual-motor neurons also appeared in suppression
560 temporal dynamics, again showing weaker suppression in the visual neurons (Fig. 4B).
561 Thus, there are differences in saccadic suppression strength between visual and visual-
562 motor SC neurons, and visual-motor neuron suppression selectivity appears more similar
563 to behavioral effects, both in our own experiments (Figs. 1-2) as well as in the literature
564 of human perceptual effects (Burr et al. 1982; Burr et al. 1994; Volkmann et al. 1978)
565 and monkey contrast detection thresholds (Hass and Horwitz 2011).
566
567 Even though our previously published results revealed no differences in post-
568 microsaccadic suppression in the SC as a function of microsaccade direction (Chen et al.
569 2015), we nonetheless analyzed movement directions in the present study as well. Across
570 our population, the direction of a microsaccade relative to the location of a neuron's RF

hotspot was fairly uniformly distributed (Fig. 5A; similar to Chen et al. 2015). This means that our results in Figs. 3, 4 above are not an artifact of biased sampling of microsaccade directions. Moreover, for each spatial frequency, and for each of either visual or visual-motor neurons, we computed the suppression index of Fig. 4, but now separately for either microsaccades towards or opposite the RF location (with "towards" and "opposite" being defined as in Chen et al. 2015). Figure 5B shows the results of this analysis for an example spatial frequency. As can be seen from the figure, for either visual or visual-motor neurons, the suppression values observed were statistically similar whether the microsaccade occurring before stimulus onset was directed towards or away from the grating location ($p=0.64$ for visual neurons and $p=0.42$ for visual-motor neurons, Wilcoxon rank sum test). This result also held for all other spatial frequencies ($p>0.07$ for either visual or visual-motor neurons, Wilcoxon rank sum test). Because of this, we combined microsaccade directions in all subsequent analyses.

Better Correlation Between Visual-Motor Neuron Dynamics and Behavior than Between Visual Neuron Dynamics and Behavior

To further explore the apparent similarity between visual-motor neuron suppression patterns (Fig. 4) and behavior (Fig. 2), we used the dynamics of our recorded population as a proxy for how the SC might be engaged in our behavioral task of Figs. 1-2. We plotted the time course of behavioral suppression (similar to Fig. 2H, K) for each spatial frequency and each monkey individually (Fig. 6A, E), and we also plotted the neural time course of visual-motor neuron suppression, again for each monkey individually (Fig. 6B, F; an example time course for purely visual neurons can also be seen in Fig. 4B). For this

comparative analysis, we used the same binning windows in both behavioral and neural data (50-ms bin widths in steps of 10 ms starting at 0 ms after microsaccade end), and we next correlated the two time courses: we plotted all samples of the behavioral time course against all samples of the neural time course irrespective of spatial frequency or time after microsaccades (Fig. 6C, G). There was high correlation between visual burst strength in SC visual-motor neurons and the behavioral effect of microsaccadic suppression: whenever visual bursts were weaker, RT costs increased, and vice versa, regardless of spatial frequency or time after microsaccades. This high correlation is particularly remarkable given that the behavioral and neural data were collected in completely different sessions and with different behavioral tasks, and even with imperfect matching of neuron locations relative to the grating location used in the behavioral study.

The highest correlation between neural patterns and behavior was observed only when we used peak visual response of visual-motor SC neurons as the behavioral predictor (Fig. 6C, G). When we correlated behavioral time courses with peak visual response of purely visual neurons, the correlations were significantly less (Fig. 6D, H; $p=0.02$ for monkey N and $p=0.02$ for monkey P, Steiger's Z-test; actual correlation values are shown in the figure). Thus, a most simple linear read-out of visual-motor neurons would fare better at predicting behavior than a similarly simple read-out of purely visual neurons.

The results of Fig. 6 suggest that saccadic suppression in visual-motor neurons is more in line with our behavioral effects than for purely visual neurons. However, one possible confound could be in the distribution of preferred spatial frequencies in visual-motor

neurons. For example, if only the preferred spatial frequency of a neuron experiences the strongest suppression, and if visual-motor neurons only had low preferred spatial frequencies, then the selective suppression of Fig. 4A would emerge, because there would be more visual-motor neurons preferring low spatial frequencies than visual neurons. However, we found no clear differences in patterns of preferred spatial frequencies between visual and visual-motor neurons. Specifically, across our population, both visual and visual-motor neurons spanned a wide range of preferred spatial frequencies (from 0.56 cpd to 4.54 cpd in visual neurons and from 0.56 cpd to 4.82 cpd in visual-motor neurons), with large overlap between the two neuron types; this meant that there was no statistically significant difference in preferred spatial frequencies between our visual and visual-motor neurons ($p=0.996$, Wilcoxon rank sum test).

To further investigate the above potential confound, we also explicitly analyzed suppression profiles of visual-motor neurons as a function of the neurons' preferred spatial frequencies. For each spatial frequency, we took only neurons preferring this spatial frequency, and we checked how these neurons were suppressed. Figure 7A-D shows the results of this analysis. There was indeed a tendency for the preferred spatial frequency of a neuron to experience the strongest suppression relative to other frequencies (e.g. black arrows). However, this strongest suppression still became progressively weaker and weaker with increasing spatial frequency (e.g. compare Fig. 7A, B to Fig. 7C, D). This is further demonstrated by Fig. 7E, in which we took the maximal suppression frequency from each of the panels in Fig. 7A-D and plotted them with an indication of the behavioral microsaccadic suppression profile (obtained as the

inverse of RT modulation profiles from Fig. 2B, E, with arbitrary y-axis scaling). Importantly, we again made sure that the neural suppression data in this figure were analyzed in an identical manner to behavioral analyses (i.e. we considered the same interval of stimulus onsets happening 20-100 ms after microsaccade end as in the behavioral analyses). As can be seen in Fig. 7E, there was a clear match between neural and behavioral effects in both animals (the correlation between neural suppression and behavioral suppression in this figure was 0.99 for monkey N and 0.89 for monkey P). Thus, the selective suppression of Figs. 3-6 was not an artifact of potential biased spatial-frequency tuning properties of only visual-motor neurons.

Taken together, our results so far suggest that spatial-frequency specific SC saccadic suppression is localized in the visual-motor neurons, with visual neurons only showing modest and non-selective suppression.

Influence of a Putative Microsaccadic Source Signal on Local SC Population Activity During Suppression

To demonstrate that there may indeed be a saccadic source signal associated with suppressed SC visual bursts (i.e. putative corollary discharge associated with the movement command), we analyzed local field potentials (LFP's) around our electrodes (Materials and Methods). Stimulus onset in no-microsaccade trials caused a negative-going "stimulus-evoked" LFP deflection for both visual and visual-motor electrode tracks (Hafed and Chen 2016; Ikeda et al. 2015). For example, Fig. 8 shows LFP traces (in a format similar to Fig. 3) as a function of spatial frequency for an example superficial

663 track (i.e. among visual neurons; Fig. 8A) and an example deeper track (among visual-
664 motor neurons; Fig. 8B). Remarkably, on microsaccade trials (unsaturated colors),
665 stimulus-evoked LFP response was not suppressed for any of the spatial frequencies. In
666 fact, for the visual-motor electrode track (Fig. 8B), LFP response was *enhanced*, and
667 more so with increasing spatial frequency (Fig. 9A; $p<0.01$, Kruskal-Wallis test on the
668 modulation index with spatial frequency as the main factor). Given that LFP's reflect not
669 just local population spiking activity, but also putative synaptic inputs, these results
670 suggest the existence of a possible microsaccade-related input modulating visual bursts.
671 This effect, of an enhanced LFP response with increasing spatial frequency, was again
672 stronger in visual-motor than visual electrode tracks, as summarized in Fig. 9A.
673 However, it is important to emphasize here that this signal was not a direct microsaccade
674 command because none of our neurons at all electrode locations in this study exhibited
675 microsaccade-related movement bursts (Materials and Methods).
676
677 Our interpretation of an increased LFP negativity as reflecting a possible movement-
678 related input mediating firing rate suppression effects is consistent with the enhanced
679 LFP response seen in Figs. 8 and 9A for high spatial frequencies. These frequencies
680 evoke the weakest visual activity (Figs. 3, 8; saturated colors). Thus, if the LFP signal
681 reflects both visual inputs associated with the stimulus onset as well as movement-related
682 modulatory inputs to the population associated with movement execution (which do not
683 depend on visual response strength), then the influence of the modulatory input (i.e. the
684 putative saccadic source signal for suppression) should become increasingly more
685 obvious in the LFP with increasing spatial frequency (Fig. 9A). However, we cannot tell

686 from this data whether the two signals integrated in the LFP reflect pure superposition of
687 visual and modulatory inputs, or whether a more complex integration takes place. In any
688 case, combined with earlier firing rate results, our LFP analyses reveal that visual-motor
689 SC neurons may be closely associated with a movement-related source for spatial-
690 frequency specific saccadic suppression.
691
692 One possible confound with the above result is that microsaccades (even though they
693 ended before stimulus onset) might cause long-lasting LFP modulations, which would be
694 superimposed on a stimulus-evoked LFP deflection in Fig. 8. In other words, the evoked
695 response could potentially still be suppressed, but it could be *level-shifted* because it rides
696 on a microsaccade-induced LFP modulation. We thus tested for intrinsic microsaccade-
697 induced LFP modulation. During simple fixation without any other visual stimuli, both
698 visual and visual-motor SC electrode locations exhibited prolonged microsaccade-related
699 LFP modulations, involving a subtle negativity after microsaccade end, as is shown in
700 Fig. 10 (additional evidence of such negativity can also be seen in the pre-stimulus
701 interval of Fig. 8, but it is washed out because of alignment to stimulus onset rather than
702 to microsaccades). So, we wondered whether this modulation is sufficient to explain the
703 lack of LFP suppression in stimulus-evoked LFP's (Fig. 8). We corrected for a baseline
704 shift at grating onset (Materials and Methods), and we still found no suppression in the
705 strength of the stimulus-evoked LFP response (Fig. 9A). Thus, in Figs. 8-10, we believe
706 that we have uncovered evidence for a putative microsaccade-related modulatory input at
707 the time of visual burst suppression in both SC visual and visual-motor neurons. This
708 input does not itself necessarily trigger microsaccades (see Discussion); it may instead

mediate visual burst suppression in firing rates, although the exact mechanisms remain to be explored. Moreover, the modulatory input shows differential modulation between superficial and intermediate electrode tracks (Fig. 9A), consistent with our firing rate results.

Enhanced stimulus-evoked LFP response amplitudes (Fig. 9A) were also accompanied by slightly faster LFP responses (Fig. 9B), again consistent with a movement-related source modulating neural firing rates at the time visual burst occurrence (because the movement happened before stimulus onset). It is also interesting to note that, like firing rate time courses, time courses of stimulus-evoked LFP modulations for stimuli appearing after microsaccades were also correlated with behavioral microsaccadic suppression dynamics (as in Fig. 6). In the LFP's, the best behavioral predictor was the latency of stimulus-evoked LFP deflection (Fig. 11, formatted similarly to Fig. 6), and visual-motor electrode tracks again showed higher correlation values with behavior (Fig. 11C, G) than visual electrode tracks (Fig. 11D, H). For monkey N, this effect was significant ($p<0.01$, Steiger's Z-test), but it did not reach significance in monkey P ($p=0.38$).

Our results combined demonstrate that visual-motor neurons are more in line with selective effects of saccadic suppression, both in humans (Burr et al. 1982; Burr et al. 1994; Volkmann et al. 1978) and monkeys (Fig. 2; also see Hass and Horwitz 2011), than purely visual neurons. This suggests that the mechanisms for saccadic suppression in the SC are more complicated than those suggested by a hypothesized pathway of a simple

731 inhibitory relay to superficial SC layers from deeper centers of the saccade motor
732 command.

Discussion

We found spatial-frequency selective saccadic suppression in SC visual-motor neurons, and the neural dynamics of visual-motor neuron suppression were well correlated with behavior. Visual neurons showed weaker suppression overall, which was also not dependent on spatial frequency. These results suggest that SC visual-motor neurons are among the neural loci for spatial-frequency specific saccadic suppression. Because spatial-frequency specificity is a robust characteristic of saccadic suppression (Burr et al. 1994; Hass and Horwitz 2011), identifying neural loci for this phenomenon is important. In what follows, we discuss our methodological choices, the implications of our results, and how these results fit within our current understanding of saccades, active vision, and the SC.

Our results are in line with interpretations of saccadic suppression as a reduction in response gain (Chen et al. 2015; Guez et al. 2013; Hafed and Krauzlis 2010). Consistent with this, we have recently found that SC neural contrast thresholds are increased after microsaccades (Chen et al. 2015). We have also found that for SC neurons possessing some baseline activity in the absence of a stimulus, there was very modest peri-microsaccadic modulation of activity (see Fig. S2 of Chen et al. 2015) when compared to the modulations in stimulus-evoked visual bursts that we have observed here and earlier (Chen et al. 2015; Hafed and Krauzlis 2010). We believe that observations like these place constraints on the potential sources and mechanisms of extra-retinal modulation often invoked in theories of saccadic suppression.

There have been few successful demonstrations of spatial-frequency specific patterns of saccadic suppression in neural activity. In early visual areas, selective magno-cellular pathway suppression is not clear (Hass and Horwitz 2011; Kleiser et al. 2004; Ramcharan et al. 2001; Reppas et al. 2002; Royal et al. 2006), even though behavioral effects strongly predicted them (Burr et al. 1982; Burr et al. 1994; Hass and Horwitz 2011; Volkmann et al. 1978). Rather, there is mild suppression, regardless of magno- or parvo-cellular pathway. Higher areas, primarily in the dorsal stream, do show saccadic suppression dynamics (Krock and Moore 2016; Zanos et al. 2016; Bremmer et al. 2009; Han et al. 2009; Ibbotson et al. 2008; Ibbotson et al. 2007; Thiele et al. 2002), but the origins of such suppression remain elusive. In fact, it has been suggested that suppression in motion-related areas MT and MST (Bremmer et al. 2009; Ibbotson et al. 2008; Ibbotson et al. 2007; Thiele et al. 2002) may be inherited from earlier visual areas (Ibbotson et al. 2008; Ibbotson et al. 2007), which themselves have weak and unselective suppression. Thus, there is a pressing need for better understanding of saccadic suppression mechanisms.

The fact that primarily motion areas have been shown to exhibit the most convincing suppression additionally does not help account for the fact that saccadic suppression may be useful for perception even if the "motion problem" (Wurtz 2008) caused by saccades, which we described in the Introduction, is solved. For example, suppression could help regularize processing of stimuli after saccades, regardless of the image shift itself. Consistent with this, we saw SC suppression for microsaccades, even though both the

779 retinal-image motion and displacement caused by these eye movements are quite mild.
780 Moreover, we saw suppression even with purely stationary gratings.
781
782 Related to the above, the fact that we saw any effects with microsaccades at all is
783 interesting in its own regard, because it adds to the microsaccade literature, but the real
784 advantage from studying microsaccades was that they allowed better experimental
785 control. Microsaccades are mechanistically similar to larger saccades (Hafed 2011; Hafed
786 et al. 2015; Hafed et al. 2009; Zuber et al. 1965), making them an extremely viable tool
787 to understanding saccadic suppression. However, these movements simplify several
788 challenges associated with large saccades. For example, studies with large saccades have
789 to contend with large image shifts caused by eye movements. As a result, full field
790 stimuli often become necessary (Ibbotson et al. 2008; Ibbotson et al. 2007). In our case,
791 we could use stimuli identical to how normal experiments might stimulate RF's. More
792 importantly, microsaccades allowed us to dissociate the location of saccadic suppression
793 from the movement endpoint location, as is known to happen with large saccades (Knoll
794 et al. 2011). This has allowed us to make the intriguing observation of movement-related
795 LFP modulations (Fig. 10) even in extra-foveal SC (i.e. with no microsaccade-related
796 bursting neurons). These modulations, similar to saccade-related LFP modulations in
797 human SC (Liu et al. 2009), can potentially explain recently observed peri-microsaccadic
798 alterations in neural activity and behavior at eccentricities much farther than
799 microsaccade amplitudes (Chen et al. 2015; Hafed 2013; Hafed et al. 2015; Tian et al.
800 2016).
801

802 Another experimental advantage here was the fact that SC shows suppression *after*
803 saccades in our type of paradigm (Chen et al. 2015; Hafed and Krauzlis 2010). This
804 allowed us to avoid probing neurons during the eye movements themselves. Of course,
805 saccadic suppression would be even stronger *during* the microsaccades themselves, as we
806 have recently shown (Chen et al. 2015; Hafed and Krauzlis 2010), which is further
807 evidence of a consistency between our visual-motor neural modulations and classic
808 perceptual effects of saccadic suppression in humans (e.g. Zuber et al. 1966). Thus, our
809 choice to focus on post-movement modulations was one of exploiting the experimental
810 advantages of doing so as opposed to one of a conceptual difference between our visual-
811 motor neural modulations and the phenomenon itself.
812
813 Concerning superficial visual neurons, one can speculate about their source of mild and
814 unselective suppression. This suppression could reflect retinal effects, because the
815 superficial SC receives retinal projections (Pollack and Hickey 1979). Indeed, retinal
816 outputs do show transient perturbations in response to saccade-like image displacements
817 (Roska and Werblin 2003). Additionally, the effect could be inherited from V1, which
818 does not show selectivity (Hass and Horwitz 2011). Regardless of the source, suppression
819 in visual neurons is not selective for spatial frequency as is known in perception (e.g.
820 Burr et al. 1994). Of course, such suppression could still be functional. For example, a
821 collicular-thalamic-cortical pathway from superficial SC may selectively target motion-
822 related areas (Berman and Wurtz 2008; 2010; 2011; Wurtz et al. 2011). As a result,
823 superficial SC may still contribute to saccadic suppression of motion (Bridgeman et al.
824 1975; Burr et al. 1982); in this case, selectively suppressing motion by superficial SC

825 neurons would arise not necessarily because the neurons themselves are selective in their
826 suppression profiles, but instead because of selectivity in their connections to cortical
827 targets. While this idea is consistent with similarities of neural saccadic suppression
828 dynamics between superficial SC neurons and MT neurons (Berman et al. 2017), it
829 receives substantially less support from SC inactivation experiments in the same study
830 (Berman et al. 2017). In these experiments, inactivating the superficial SC did not reduce
831 MT suppression effects, whereas inactivating the deeper SC layers did. In this regard, we
832 believe that the pathway from intermediate SC layers to FEF via thalamus (Sommer and
833 Wurtz 2004) is the more likely source of cortical saccadic suppression in general, not
834 only in MT, but also in other cortical areas like FEF (Krock and Moore 2016) and V4
835 (Han et al. 2009; Zanos et al. 2016). This is consistent with our present results showing
836 that saccadic suppression may already be established in the intermediate SC layers
837 themselves without the need for an internal inhibitory relay to superficial layers. This
838 inhibitory relay (Isa and Hall 2009; Lee et al. 2007; Phongphanphanee et al. 2011) could
839 be used for other functions, perhaps in coordination with an excitatory relay in parallel,
840 which has also been identified (Ghitani et al., 2014).
841
842 Our observation of a lack of suppression selectivity in purely visual neurons also helps
843 address an important question regarding the nature of our selective visual-motor neuron
844 modulations. Specifically, it may be argued that (peripheral) SC neurons may
845 preferentially over-sample low spatial frequencies in their tuning curves (Hafed and Chen
846 2016), meaning that they exhibit higher sensitivity for low spatial frequencies even
847 without microsaccades. This, in turn, could mean that we only saw stronger suppression

848 at low spatial frequencies (in the visual-motor neurons) simply because the baseline
849 visual responses were stronger. However, our visual neurons preferred similar ranges of
850 spatial frequencies as our visual-motor neurons. If our effects are explained by the
851 dependence of suppression on baseline visual sensitivity in the absence of microsaccades,
852 then our visual neurons should have shown the same patterns of selective suppression as
853 the visual-motor neurons, but they did not (Figs. 3, 4). Second, we specifically examined
854 suppression within each spatial frequency relative to the no-microsaccade baseline of the
855 same frequency, in order to isolate the suppression effect independent of baseline
856 response strength. This avoided questions of absolute firing sensitivity across spatial
857 frequencies. Third, in Fig. 7, we explicitly examined suppression as a function of
858 preferred spatial frequency and still found diminishing returns in suppression strength
859 with increasing spatial frequency even when each spatial frequency bin only included the
860 neurons preferring that frequency. Finally, because the visual system is inherently
861 generally low pass anyway (especially in the periphery), then even a mechanism in which
862 suppression simply scales with visual sensitivity of a given spatial frequency would still
863 explain the well known perceptual phenomenon of selective suppression of low spatial
864 frequencies in humans.
865
866 There may also be an additional potential counter-interpretation of our results.
867 Specifically, it may be argued that we uncovered a highly specific effect only modulating
868 saccadic RT's, and that SC modulations are irrelevant for other forms of behavior (e.g.
869 not requiring saccadic responses). However, this is unlikely. First, the SC contributes to
870 behavior even with non-saccadic outputs. For example, during attentional tasks with

871 button presses, SC lesions impair performance (Sapir et al. 1999), suggesting that it is
872 sensory and/or cognitive modulations that are relevant. Consistent with this, the SC
873 contributes to attentional paradigms with a variety of response modalities (Lovejoy and
874 Krauzlis 2010; Zenon and Krauzlis 2012). Second, we only looked at the earliest visual
875 responses and uncovered strong correlations to behavior observed in separate
876 experiments. This indicates that it was the sensory response that mattered. Consistent
877 with this, we have recently found that the occurrence of a microsaccade near the time of
878 stimulus onset affected both manual and saccadic RT's in a similar fashion despite the
879 different motor response modalities (Tian et al. 2016). Third, our behavioral effects on
880 RT are themselves remarkably similar to perceptual effects of saccadic suppression in
881 humans, but using different perceptual measures and response modalities (Burr et al.
882 1982; Burr et al. 1994; Volkmann et al. 1978). Fourth, we found that monkey P had a
883 stronger suppression effect in behavior than monkey N at the low spatial frequencies
884 (compare the cyan curves in Fig. 2H and Fig. 2K) even though monkey P had
885 significantly longer saccadic RT's to begin with (compare the black no-microsaccade
886 curves in Fig. 2A and Fig. 2D). If our behavioral and neural effects were restricted to
887 limits on saccadic RT, perhaps due to potential saccadic refractory periods between
888 successive saccades and microsaccades, then monkey P should have shown weaker
889 behavioral suppression than monkey N since this monkey's saccadic system had plenty of
890 time to recover from the previous generation of a microsaccade before having to generate
891 the next saccadic RT. Given all of the above, and further arguments in (Hafed and
892 Krauzlis 2010), we find it unlikely that our modulations are only specific to modulating
893 saccadic RT's.

If that is the case, then why might the SC be among the neural substrates for spatial-frequency specific saccadic suppression? We think that the SC has several appealing features to place it well within a hypothetical saccadic suppression system. For example, the SC contributes to triggering the saccade command. Thus, a source of corollary discharge is already present in the visual-motor layers, as demonstrated by our differential firing rate (Figs. 3-7) and LFP (Figs. 8-10) effects. Second, proximity of the SC to motor outputs confers an additional advantage: SC suppression, besides having potential perceptual effects, could help to regularize how often subsequent saccades are made to sample the visual world. That is, in reality, suppression could serve to control the temporal structure of saccades, which can be very important both behaviorally (Tian et al. 2016) and cortically (Lowet et al. 2016). This becomes even more interesting in light of the strong prevalence of low spatial frequencies in natural scene statistics (Field 1987), suggesting that selective suppression of low spatial frequencies is indeed functional. Moreover, controlling the temporal structure of saccades might explain refractory periods between successive movements, which we briefly alluded to above. Specifically, it is known that signal delays from the retina to the eye muscles can be much shorter than typically observed inter-saccadic intervals. For example, SC neurons receive visual responses within ~50 ms after stimulus onset, and SC stimulation can trigger saccades within ~20 ms (i.e. a total of ~70 ms); on the other hand, typical RT values or inter-saccadic intervals are at least twice as long (Wurtz and Mohler 1976; Schiller and Stryker 1972; Robinson 1972; Boch et al. 1984). This has led to talk of saccadic refractory periods (e.g. Becker and Jurgens 1979), but the mechanisms for such refractory periods

are not known. If the SC is desensitized after every saccade, then this can delay subsequent saccades, introducing refractoriness, and also more generally controlling the temporal structure of eye movement generation.

Acknowledgements

We were funded by the Werner Reichardt Centre for Integrative Neuroscience (CIN) at the Eberhard Karls University of Tübingen. The CIN is an Excellence Cluster funded by the Deutsche Forschungsgemeinschaft (DFG) within the framework of the Excellence Initiative (EXC 307).

928 **References**

929

930 **Becker W, and Jurgens R**. An analysis of the saccadic system by means of double step
931 stimuli. *Vision Res* 19: 967-983, 1979.
932 **Berman RA, Cavanaugh J, McAlonan K, and Wurtz RH**. A circuit for saccadic
933 suppression in the primate brain. *J Neurophysiol* IN PRESS, doi:10.1152/jn.00679.2016
934 **Berman RA, and Wurtz RH**. Exploring the pulvinar path to visual cortex. *Prog Brain*
935 *Res* 171: 467-473, 2008.
936 **Berman RA, and Wurtz RH**. Functional identification of a pulvinar path from superior
937 colliculus to cortical area MT. *J Neurosci* 30: 6342-6354, 2010.
938 **Berman RA, and Wurtz RH**. Signals conveyed in the pulvinar pathway from superior
939 colliculus to cortical area MT. *J Neurosci* 31: 373-384, 2011.
940 **Boch R, Fischer B, and Ramsperger E**. Express-saccades of the monkey: reaction times
941 versus intensity, size, duration, and eccentricity of their targets. *Exp Brain Res* 55: 223-
942 231, 1984.
943 **Boehnke SE, and Munoz DP**. On the importance of the transient visual response in the
944 superior colliculus. *Curr Opin Neurobiol* 18: 544-551, 2008.
945 **Breitmeyer BG**. Simple reaction time as a measure of the temporal response properties
946 of transient and sustained channels. *Vision Res* 15: 1411-1412, 1975.
947 **Bremmer F, Kubischik M, Hoffmann KP, and Krekelberg B**. Neural dynamics of
948 saccadic suppression. *J Neurosci* 29: 12374-12383, 2009.
949 **Bridgeman B, Hendry D, and Stark L**. Failure to detect displacement of the visual
950 world during saccadic eye movements. *Vision Res* 15: 719-722, 1975.

Burr DC, Holt J, Johnstone JR, and Ross J. Selective depression of motion sensitivity during saccades. *J Physiol* 333: 1-15, 1982.

Burr DC, Morrone MC, and Ross J. Selective suppression of the magnocellular visual pathway during saccadic eye movements. *Nature* 371: 511-513, 1994.

Burr DC, and Ross J. Contrast sensitivity at high velocities. *Vision Res* 22: 479-484, 1982.

Campbell FW, and Wurtz RH. Saccadic omission: why we do not see a grey-out during a saccadic eye movement. *Vision Res* 18: 1297-1303, 1978.

Castet E, Jeanjean S, and Masson GS. 'Saccadic suppression'- no need for an active extra-retinal mechanism. *Trends Neurosci* 24: 316-318, 2001.

Castet E, and Masson GS. Motion perception during saccadic eye movements. *Nat Neurosci* 3: 177-183, 2000.

Chen CY, and Hafed ZM. Postmicrosaccadic enhancement of slow eye movements. *J Neurosci* 33: 5375-5386, 2013.

Chen CY, Ignashchenkova A, Thier P, and Hafed ZM. Neuronal response gain enhancement prior to microsaccades. *Curr Biol* 25: 2065-2074, 2015.

Diamond MR, Ross J, and Morrone MC. Extraretinal control of saccadic suppression. *J Neurosci* 20: 3449-3455, 2000.

Field DJ. Relations between the statistics of natural images and the response properties of cortical cells. *J Opt Soc Am A* 4: 2379-2394, 1987.

Fischer B, and Boch R. Saccadic eye movements after extremely short reaction times in the monkey. *Brain Res* 260: 21-26, 1983.

Fuchs AF, and Robinson DA. A method for measuring horizontal and vertical eye movement chronically in the monkey. *J Appl Physiol* 21: 1068-1070, 1966.

Garcia-Perez MA, and Peli E. Visual contrast processing is largely unaltered during saccades. *Front Psychol* 2: 247, 2011.

Ghitani N, Bayguinov PO, Vokoun CR, McMahon S, Jackson MB, and Basso MA. Excitatory synaptic feedback from the motor layer to the sensory layers of the superior colliculus. *J Neurosci* 34:6822-6833, 2014.

Guez J, Morris AP, and Krekelberg B. Intrasaccadic suppression is dominated by reduced detector gain. *J Vis* 13: 2013.

Hafed ZM. Alteration of visual perception prior to microsaccades. *Neuron* 77: 775-786, 2013.

Hafed ZM. Mechanisms for generating and compensating for the smallest possible saccades. *Eur J Neurosci* 33: 2101-2113, 2011.

Hafed ZM, and Chen C-Y. Sharper, stronger, faster upper visual field representation in primate superior colliculus. *Curr Biol* 26: 1647-1658, 2016.

Hafed ZM, Chen C-Y, and Tian X. Vision, perception, and attention through the lens of microsaccades: mechanisms and implications. *Front Sys Neurosci* 9: 167, 2015.

Hafed ZM, Goffart L, and Krauzlis RJ. A neural mechanism for microsaccade generation in the primate superior colliculus. *Science* 323: 940-943, 2009.

Hafed ZM, and Ignashchenkova A. On the dissociation between microsaccade rate and direction after peripheral cues: microsaccadic inhibition revisited. *J Neurosci* 33: 16220-16235, 2013.

Hafed ZM, and Krauzlis RJ. Microsaccadic suppression of visual bursts in the primate superior colliculus. *J Neurosci* 30: 9542-9547, 2010.

Hafed ZM, and Krauzlis RJ. Similarity of superior colliculus involvement in microsaccade and saccade generation. *J Neurophysiol* 107: 1904-1916, 2012.

Han X, Xian SX, and Moore T. Dynamic sensitivity of area V4 neurons during saccade preparation. *Proc Natl Acad Sci U S A* 106: 13046-13051, 2009.

Hass CA, and Horwitz GD. Effects of microsaccades on contrast detection and V1 responses in macaques. *J Vis* 11: 1-17, 2011.

Ibbotson MR, Crowder NA, Cloherty SL, Price NS, and Mustari MJ. Saccadic modulation of neural responses: possible roles in saccadic suppression, enhancement, and time compression. *J Neurosci* 28: 10952-10960, 2008.

Ibbotson MR, and Krekelberg B. Visual perception and saccadic eye movements. *Curr Opin Neurobiol* 21: 553-558, 2011.

Ibbotson MR, Price NS, Crowder NA, Ono S, and Mustari MJ. Enhanced motion sensitivity follows saccadic suppression in the superior temporal sulcus of the macaque cortex. *Cereb Cortex* 17: 1129-1138, 2007.

Ikeda T, Boehnke SE, Marino RA, White BJ, Wang CA, Levy R, and Munoz DP. Spatio-temporal response properties of local field potentials in the primate superior colliculus. *Eur J Neurosci* 41: 856-865, 2015.

Ilg UJ, and Hoffmann KP. Motion perception during saccades. *Vision Res* 33: 211-220, 1993.

Isa T, and Hall WC. Exploring the superior colliculus in vitro. *J Neurophysiol* 102: 2581-2593, 2009.

Judge SJ, Richmond BJ, and Chu FC. Implantation of magnetic search coils for measurement of eye position: an improved method. *Vision Res* 20: 535-538, 1980.

Kleiser R, Seitz RJ, and Krekelberg B. Neural correlates of saccadic suppression in humans. *Curr Biol* 14: 386-390, 2004.

Knoll J, Binda P, Morrone MC, and Bremmer F. Spatiotemporal profile of peri-saccadic contrast sensitivity. *J Vis* 11: 1-12, 2011.

Krock RM, and Moore T. Visual sensitivity of frontal eye field neurons during the preparation of saccadic eye movements. *J Neurophysiol* doi: 10.1152/jn.01140.2015, 2016.

Lee PH, Sooksawate T, Yanagawa Y, Isa K, Isa T, and Hall WC. Identity of a pathway for saccadic suppression. *Proc Natl Acad Sci U S A* 104: 6824-6827, 2007.

Li X, and Basso MA. Preparing to move increases the sensitivity of superior colliculus neurons. *J Neurosci* 28: 4561-4577, 2008.

Liu X, Nachev P, Wang S, Green A, Kennard C, and Aziz T. The saccade-related local field potentials of the superior colliculus: a functional marker for localizing the periventricular and periaqueductal gray. *J Clin Neurophysiol* 26: 280-287, 2009.

Lovejoy LP, and Krauzlis RJ. Inactivation of primate superior colliculus impairs covert selection of signals for perceptual judgments. *Nat Neurosci* 13: 261-266, 2010.

Lowet E, Roberts MJ, Bosman CA, Fries P, and De Weerd P. Areas V1 and V2 show microsaccade-related 3-4-Hz covariation in gamma power and frequency. *Eur J Neurosci* 43: 1286-1296, 2016.

Matin E. Saccadic suppression: a review and an analysis. *Psychol Bull* 81: 899-917, 1974.

Matin E, Clymer AB, and Matin L. Metacontrast and saccadic suppression. *Science* 178: 179-182, 1972.

Phongphanphanee P, Mizuno F, Lee PH, Yanagawa Y, Isa T, and Hall WC. A circuit model for saccadic suppression in the superior colliculus. *J Neurosci* 31: 1949-1954, 2011.

Pollack JG, and Hickey TL. The distribution of retino-collicular axon terminals in rhesus monkey. *J Comp Neurol* 185: 587-602, 1979.

Rajkai C, Lakatos P, Chen CM, Pincze Z, Karmos G, and Schroeder CE. Transient cortical excitation at the onset of visual fixation. *Cereb Cortex* 18: 200-209, 2008.

Ramcharan EJ, Gnadt JW, and Sherman SM. The effects of saccadic eye movements on the activity of geniculate relay neurons in the monkey. *Vis Neurosci* 18: 253-258, 2001.

Reppas JB, Usrey WM, and Reid RC. Saccadic eye movements modulate visual responses in the lateral geniculate nucleus. *Neuron* 35: 961-974, 2002.

Robinson DA. Eye movements evoked by collicular stimulation in the alert monkey. *Vision Res* 12: 1795-1808, 1972.

Roska B, and Werblin F. Rapid global shifts in natural scenes block spiking in specific ganglion cell types. *Nat Neurosci* 6: 600-608, 2003.

Ross J, Burr D, and Morrone C. Suppression of the magnocellular pathway during saccades. *Behav Brain Res* 80: 1-8, 1996.

Royal DW, Sary G, Schall JD, and Casagrande VA. Correlates of motor planning and postsaccadic fixation in the macaque monkey lateral geniculate nucleus. *Exp Brain Res* 168: 62-75, 2006.

Sapir A, Soroker N, Berger A, and Henik A. Inhibition of return in spatial attention: direct evidence for collicular generation. *Nat Neurosci* 2: 1053-1054, 1999.

Schiller PH, and Stryker M. Single-unit recording and stimulation in superior colliculus of the alert rhesus monkey. *J Neurophysiol* 35: 915-924, 1972.

Sommer MA, and Wurtz RH. What the brain stem tells the frontal cortex. I. Oculomotor signals sent from superior colliculus to frontal eye field via mediodorsal thalamus. *J Neurophysiol* 91: 1381-1402, 2004.

Sperry RW. Neural basis of the spontaneous optokinetic response produced by visual inversion. *J Comp Physiol Psychol* 43: 482-489, 1950.

Thiele A, Henning P, Kubischik M, and Hoffmann KP. Neural mechanisms of saccadic suppression. *Science* 295: 2460-2462, 2002.

Tian X, Yoshida M, and Hafed ZM. A microsaccadic account of attentional capture and inhibition of return in Posner cueing. *Front Sys Neurosci* 10: 23, 2016.

Volkmann FC, Riggs LA, White KD, and Moore RK. Contrast sensitivity during saccadic eye movements. *Vision Res* 18: 1193-1199, 1978.

von Holst E, and Mittelstaedt H. Das Reafferenzprincip: Wechselwirkungen zwischen Zentralnervensystem und Peripherie. *Naturwissenschaften* 37: 464-476, 1950.

Wurtz RH. Neuronal mechanisms of visual stability. *Vision Res* 48: 2070-2089, 2008.

Wurtz RH, Joiner WM, and Berman RA. Neuronal mechanisms for visual stability: progress and problems. *Phil Trans Roy Soc London B* 366: 492-503, 2011.

Wurtz RH, and Mohler CW. Organization of monkey superior colliculus: enhanced visual response of superficial layer cells. *J Neurophysiol* 39: 745-765, 1976.

Zanos TP, Mineault PJ, Guitton D, and Pack CC. Mechanisms of saccadic suppression in primate cortical area V4. *J Neurosci* 36: 9227-9239, 2016.

Zenon Z, and Krauzlis RJ. Attention deficits without cortical neuronal deficits. *Nature* 489: 434-437, 2012.

Zuber BL, Stark L, and Cook G. Microsaccades and the velocity-amplitude relationship for saccadic eye movements. *Science* 150: 1459-1460, 1965.

Zuber BL, Stark L, and Lorber M. Saccadic suppression of the pupillary light reflex. *Exp Neurol* 14: 351-370, 1966.

Figure Legends

Figure 1 Behavioral measure of microsaccadic suppression across spatial frequencies. (**A**) Eye position (left) and radial eye velocity (right) traces from 100 sample trials from monkey N during a stimulus detection task. A 1.11 cpd grating appeared during fixation either with no nearby microsaccades (black, n=50 randomly selected trials) or ~20-100 ms after microsaccades (gray, n=50 randomly selected trials), and the monkey had to orient as fast as possible to the grating. Reaction time (RT) on the microsaccade trials was slower than on the no-microsaccade trials. Note that we flipped the gray position and velocity traces around the horizontal axis to facilitate comparison to the black traces, and we also displaced the initial fixation position in the position traces. The microsaccades are more visible in the velocity traces, because they constitute spikes of eye velocity. (**B**) Same analysis, but from 100 randomly selected trials having a higher spatial-frequency grating (4.44 cpd). RT's in this case were more similar between the microsaccade and no-microsaccade trials, suggesting that the effect in **A** disappears with increasing spatial frequency. (**C**) Similar observations to **B** were also made for 11.11 cpd gratings. Note that RT's in this case were longer than in **A** and **B**, meaning that some traces were truncated in the figure either before saccade onset or midway through saccades. Also, note that results of statistical tests for this and other figures are detailed in the text.

Figure 2 Spatial-frequency selective microsaccadic suppression in behavior. (**A**) Mean RT as a function of spatial frequency. On no-microsaccade trials (black), RT increased with spatial frequency, consistent with dependence of visual response dynamics on

spatial frequency (Breitmeyer 1975). If the same gratings appeared ~20-100 ms after microsaccades (gray), RT increased relative to no-microsaccade trials (a behavioral correlate of suppressed visual sensitivity), but more dramatically for low rather than high spatial frequencies (compare gray to black curves at different spatial frequencies). (**B**) Difference in RT between microsaccade and no-microsaccade trials (i.e. difference between gray and black curves in **A**), demonstrating the diminishing effects of microsaccades on RT behavioral costs with increasing spatial frequency. (**C**) Difference in the likelihood of express RT trials between microsaccade and no-microsaccade trials, demonstrating diminishing effects of microsaccades on reducing the likelihood of express RT's. (**D-F**) Same analyses as **A-C** but for a second monkey. (**G, H**) Time courses of mean RT (**G**; like in **A**) or difference in RT (**H**; like in **B**) as a function of the time of grating onset after microsaccade end. The figure shows time courses from two sample spatial frequencies (complete time courses from all spatial frequencies, and for each animal individually, are also shown in Fig. 6). For the difference in RT time course, RT's on trials with no microsaccades within <250 ms from grating onset were taken as the baseline. The initial RT cost caused by microsaccades was weaker for higher spatial frequency gratings (compare vertical arrows, consistent with **A**). (**I**) Likelihood of express RT trials as a function of time after microsaccade end, for the same spatial frequencies as in **G**, **H**. Immediately after microsaccades, there was an express RT cost (i.e. fewer express RT's), with gradual recovery in time. Moreover, the recovery dynamics were different for different spatial frequencies, like with overall RT (**G**, **H**). Also note that the baseline fraction of express RT's (i.e. long after microsaccades) was different for different spatial frequencies, so that the recovery for different spatial

frequencies is towards different absolute values (like in **G**). (**J-L**) Same analyses as **G-I** but for a second monkey. n=8153 trials for monkey N, and n=7117 for monkey P. Error bars, when visible, denote s.e.m.

Figure 3 Spatial-frequency selective microsaccadic suppression of visual-motor SC neurons. (**A**) Neural activity as a function of time after grating onset for two sample purely visual SC neurons (one per row). Each panel in a row shows activity after presentation of a specific spatial frequency (indicated above each panel). Rasters above each firing rate curve show individual action potentials emitted by the neuron across individual trials. We divided trials into ones in which there was no microsaccade within <100 ms from grating onset (saturated blue; n>=38 trials per spatial frequency in these sample neurons) and ones in which the grating appeared immediately after microsaccades (unsaturated blue; n>=30 trials per spatial frequency). The y-axis was scaled in each panel such that the no-microsaccade firing rates visually appeared to have approximately similar heights across panels, allowing easier comparison of suppression effects. Both neurons showed moderate microsaccadic suppression, with no clear pattern across spatial frequencies. (**B**) Same format as **A**, but for two sample visual-motor neurons. The neurons showed stronger suppression at the lowest spatial frequency, and the suppression gradually decreased in strength with increasing spatial frequency (like in behavior); by 4.44 and 11.11 cpd, there was no suppression left. For these neurons, n>=28 trials per spatial frequency for no microsaccade trials (saturated red), and n>=22 trials per spatial frequency trials for microsaccade trials (unsaturated red). Error bars denote s.e.m.

Figure 4 Spatial-frequency dependent microsaccadic suppression of visual bursts in visual-motor but not visual SC neurons. (**A**) We measured peak stimulus-evoked visual burst after grating onset (e.g. from traces like those in Fig. 3) and plotted it as a function of grating spatial frequency. We grouped neurons as purely visual (blue) or visual-motor (red). Visual neurons showed only ~10% suppression, and there was no consistent spatial-frequency dependence of this suppression. Visual-motor neurons showed ~25% suppression in the low spatial frequencies, and this effect gradually decreased with increasing spatial frequency (as in behavior). Error bars denote s.e.m. Note that the error bars for the highest spatial frequency were larger than other frequencies because some neurons completely stopped responding at 11.11 cpd, which reduced population size in this spatial frequency (Materials and Methods). (**B**) Time courses of microsaccadic suppression in visual (left) and visual-motor (right) neurons for a sample spatial frequency. We performed an analysis similar to that described in (Chen et al. 2015) but aligning on microsaccade end. For each time window after microsaccade end in which a grating appeared (x-axis; 50-ms bins in 10-ms steps), we measured peak firing rate evoked by grating onset (Materials and Methods), and we normalized it by peak firing rate on no-microsaccade trials. Visual-motor neurons showed stronger suppression than visual neurons (compare y-axis in both panels), and both neuron types experienced recovery with increasing time after microsaccades (consistent with behavioral effects). Note that the time course of visual-motor neuron suppression is similar to the time course of behavioral effects (e.g. Fig. 2H, K) and also similar to the time course of saccadic suppression in the earlier literature (e.g. Ibbotson and Krekelberg 2011; Hafed and Krauzlis 2010; Diamond et al. 2000). Figure 6 shows individual monkey time courses,

other spatial frequencies, as well as relationships between neural time courses and the respective monkey's behavioral performance dynamics. n=66 visual-motor neurons, and n=24 visual neurons.

Figure 5 Lack of dependence of microsaccadic suppression on movement direction. (**A**) Normalized histogram of microsaccade directions relative to stimulus location (i.e. with all neuronal hotspot locations rotated to be aligned with 0 as in Chen et al. 2015). Across our population, microsaccade directions were evenly distributed relative to the location of the RF stimulus, similar to the results of (Chen et al. 2015). Thus, our results from Fig. 4 are not due to biased sampling of microsaccade directions. (**B**) For each visual (left) or visual-motor (right) neuron, we calculated a suppression index (as in Fig. 4) but only for trials in which a microsaccade was directed either towards (magenta) or opposite (green) the location of the stimulus. Towards and opposite microsaccades were defined as in (Chen et al. 2015). Across the population of either visual or visual-motor neurons, the suppression index was similar for towards and opposite microsaccades, suggesting that suppression was not dependent on movement direction. Similar observations were made with large saccades in (Knoll et al. 2011). Each panel shows the p-value obtained from a rank sum test comparing neural suppression indices for towards and opposite trials. Note that we also repeated the analysis shown in this panel for all other spatial frequencies (and for either visual or visual-motor neurons), and we always obtained similar suppression values for towards and opposite microsaccades ($p>0.07$ for each performed test).

Figure 6 Correlating behavioral microsaccadic suppression with neural microsaccadic suppression on completely different experimental sessions. (**A**) Time course of difference in RT from baseline (e.g. Fig. 2H, K; Materials and Methods) as a function of time of grating onset after microsaccade end in our behavioral experiments (monkey N). Different curves show different spatial frequencies. Immediately after microsaccades, there was a strong cost in RT for low spatial frequencies, and a more moderate cost for high spatial frequencies. In all spatial frequencies, the RT cost associated with microsaccadic suppression slowly dissipated in time. (**B**) Similar analysis but for the peak visual response in our neural experiments, on completely different sessions from the behavioral data, and only for visual-motor neurons. (**C**) Correlation between the data points in **A** and those in **B**, regardless of time or spatial frequency. There was strong correlation between visual burst strength and RT cost, even on completely different experimental sessions, suggesting that visual-motor neurons are modulated during microsaccadic suppression in a manner that could be relevant for the phenomenon of (Burr et al. 1994). (**D**) Here, we correlated the behavioral points in **A** with similar points but for visual neuron time courses (e.g. Fig. 4B). The correlation with behavior was worse than in visual-motor neurons. (**E-H**) Similar observations for a second monkey. n=24 visual-motor neurons for monkey N, and n=42 visual-motor neurons for monkey P; n=15 visual neurons for monkey N, and n=9 visual neurons for monkey P.

Figure 7 Selective low-frequency suppression in visual-motor neurons independent of preferred spatial frequency. (**A-D**) In each panel, we selected only neurons preferring a single spatial frequency on no-microsaccade trials (Materials and Methods). We then

repeated the analysis of Fig. 4A. The preferred spatial frequency tended to experience the strongest suppression compared to other spatial frequencies (black arrows). However, the strength of the suppression even for the preferred spatial frequency consistently decreased with increasing spatial frequency (compare the arrows in the individual panels). Note that we did not have neurons preferring 11.11 cpd in this analysis, and we thus do not show this spatial frequency in this figure. (**E**) We collected the maximally suppressed spatial frequency from each panel in **A**-**D** (legend), and we plotted them together. The black and gray lines are a copy of the behavioral RT microsaccadic suppression curves of Fig. 2B, E, but inverted (and with arbitrary y-axis scaling) to match the neural suppression curves. As can be seen, even if the preferred spatial frequency of neurons always experienced maximal suppression, this maximal suppression was still decreased with increasing spatial frequency. Thus, the spatial-frequency selectivity of visual-motor neural suppression was still correlated with behavior. Error bars denote s.e.m. n=26, 19, 8, and 5 neurons in each of **A**, **B**, **C**, and **D**.

Figure 8 Local field potential modulations during microsaccadic suppression. This figure is formatted similarly to Fig. 3, except that we now plot LFP modulations around a sample electrode track near visual (**A**) or visual-motor (**B**) neurons. There was *no* evidence of a reduced LFP evoked response for trials with grating onset after microsaccades (faint colors). If anything, the peak evoked response, and the latency to evoked response were stronger and shorter, respectively (see Fig. 9). This effect was not explained by an intrinsic peri-microsaccadic modulation of LFP (see Figs. 9A, 10), but it is consistent with an additional movement-related modulatory signal associated with

saccade execution that influences stimulus-evoked spiking activity. Error bars denote s.e.m. For the visual track (**A**), n>=113 trials per spatial frequency on no-microsaccade trials (saturated blue), and n>=25 trials per spatial frequency on microsaccade trials (unsaturated blue). For the visual-motor track (**B**), n>=140 trials per spatial frequency on no-microsaccade trials (saturated red), and n>=12 trials on microsaccade trials (unsaturated red).

Figure 9 Lack of microsaccadic suppression in LFP stimulus-evoked responses. (**A**) We performed an analysis similar to that in Fig. 4A but on LFP's. We measured peak LFP response with and without microsaccades, and we then obtained a modulation index (Materials and Methods). The inset shows the modulation index from raw measurements, and the main panel shows the same analysis but after subtracting a baseline shift from the microsaccade trials. Specifically, Fig. 10 suggests that there is a negativity in LFP's after microsaccades, and stimulus onset in the microsaccade trials came after a previous microsaccade. Thus, we measured the peak LFP stimulus-evoked response on microsaccade trials as the difference between the raw LFP stimulus-evoked negativity minus the baseline LFP value that was present at the time of grating onset (Materials and Methods). In both the inset and the main panel, there was no suppression in the stimulus-evoked LFP response, contrary to firing rate results (Fig. 4A). Rather, there was response enhancement, which progressively increased with increasing spatial frequency, and this happened for both visual and visual-motor electrode track locations ($p<0.01$ for either baseline-corrected or raw measurements and for each of visual-only or visual-motor electrode tracks; Kruskal-Wallis test with spatial frequency as the main factor). (**B**)

Similar analyses but measuring the latency to LFP stimulus-evoked response, which decreased on microsaccade trials (y-axis values <0 ms; $p<0.02$ for visual electrode tracks and $p=0.07$ for visual-motor electrode tracks; Kruskal-Wallis test with spatial frequency as the main factor). Thus, when a stimulus appeared immediately after a microsaccade, the stimulus-evoked LFP response started earlier than without a microsaccade. Error bars denote s.e.m.

Figure 10 Microsaccade-related local field potential modulations in the absence of an RF stimulus. We aligned LFP activity to either microsaccade onset (magenta) or microsaccade end (orange) during a baseline fixation interval with no RF stimulus at all (Materials and Methods). The black curves show LFP activity during equally-long control intervals, again with no RF stimulus, but also with no microsaccade occurrence. Even though there was no microsaccade-related spiking at all the sites investigated in this study, microsaccades caused systematic modulations in both visual (**A**) and visual-motor (**B**) electrode locations in the SC, even though our electrodes were primarily placed in extra-foveal SC representations far from the movement endpoints. Thus, these LFP modulations, similar to previously reported saccade-related LFP modulations (Liu et al. 2009), reflect a potential microsaccade-related modulatory signal that can mediate microsaccadic suppression of firing rates in extra-foveal SC neurons. Also, note how the effect on visual-motor layers (**B**) is more systematic and robust than in visual layers (**A**). This is further evidence of a putative extra-retinal signal in the SC visual-motor layers that might mediate saccadic suppression (and explain Fig. 6), and it also makes it unlikely

1302 that the LFP modulations in this figure are due to ocular muscle artifacts. Error bars
1303 denote s.e.m. n=66 electrode tracks for (**B**), and n=24 electrode tracks for (**A**).
1304
1305 **Figure 11** Correlation between LFP modulation parameters and behavioral effects of
1306 suppression. This figure is formatted similarly to Fig. 6, except that here we plotted LFP
1307 time courses instead of firing rate time courses. Specifically, in **B** and **F**, we plotted the
1308 time course of LFP stimulus-evoked response latency (e.g. Fig. 9B) as a function of
1309 spatial frequency and time after microsaccades. The correlation between this latency in
1310 visual-motor layers and behavior was better (**C, G**) than in visual layers (**D, H**). Thus, it
1311 is again the visual-motor layers that are better predictors of behavior, like in Fig. 6,
1312 although firing rates (Fig. 6) showed higher correlations to behavior in general. Note that
1313 we also measured correlations between behavior and LFP stimulus-evoked response
1314 strength rather latency (data not shown), but the LFP response latency always showed the
1315 better correlations with behavior.
1316

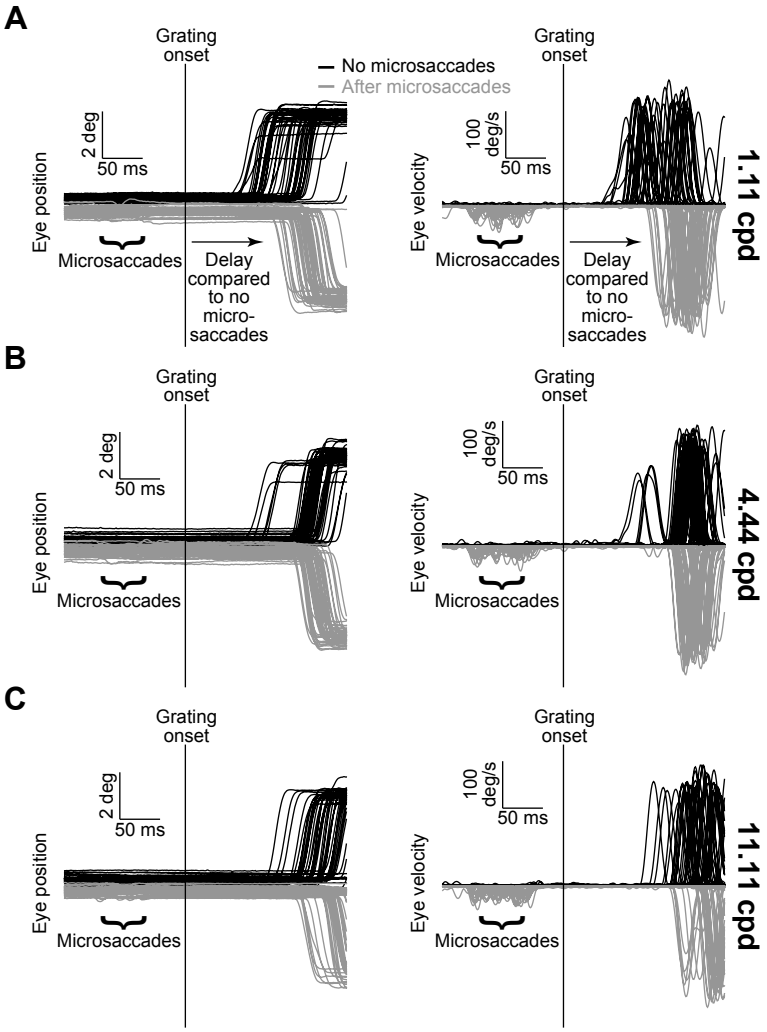
A
Grating onset
No microsaccades
After microsaccades
2 deg
50 ms
Eye position
Microsaccades
Delay compared to no micro-saccades
100 deg/s
50 ms
Eye velocity
1.11 cpd
B
4.44 cpd
C
11.11 cpd

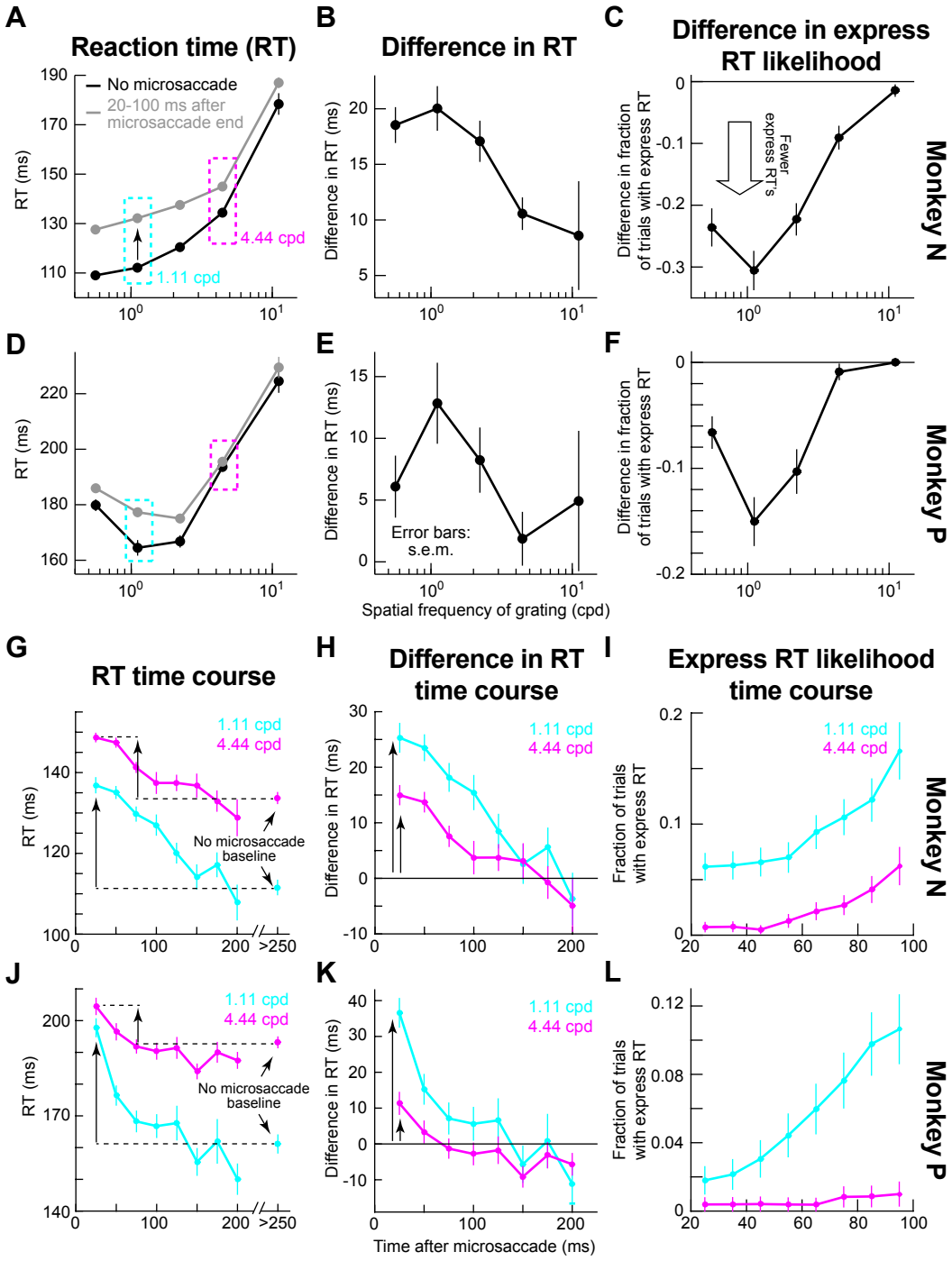
A
Reaction time (RT)
No microsaccade
20-100 ms after microsaccade end
RT (ms)
4.44 cpd
1.11 cpd
B
Difference in RT
Difference in RT (ms)
C
Difference in express RT likelihood
Difference in fraction of trials with express RT
Fewer express RT's
Monkey N
D
RT (ms)
E
Difference in RT (ms)
Error bars: s.e.m.
Spatial frequency of grating (cpd)
F
Difference in fraction of trials with express RT
Monkey P
G
RT time course
1.11 cpd
4.44 cpd
RT (ms)
No microsaccade baseline
H
Difference in RT time course
Difference in RT (ms)
I
Express RT likelihood time course
Fraction of trials with express RT
Monkey N
J
RT (ms)
No microsaccade baseline
K
Difference in RT (ms)
Time after microsaccade (ms)
L
Fraction of trials with express RT
Monkey P

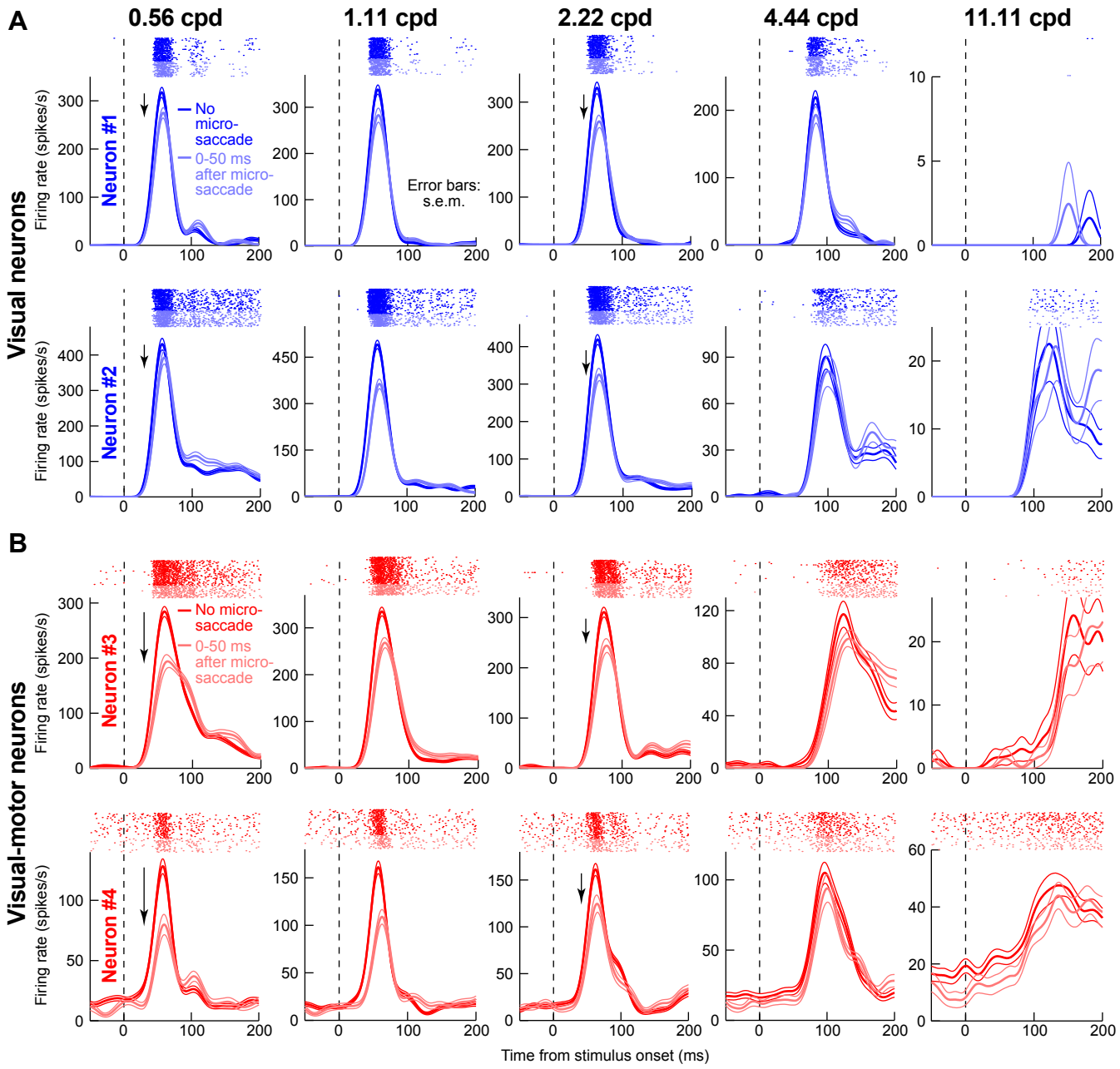
A
0.56 cpd
1.11 cpd
2.22 cpd
4.44 cpd
11.11 cpd
Visual neurons
Neuron #1
Neuron #2
Firing rate (spikes/s)
No micro-saccade
0-50 ms after micro-saccade
Error bars: s.e.m.
B
Visual-motor neurons
Neuron #3
Neuron #4
Time from stimulus onset (ms)

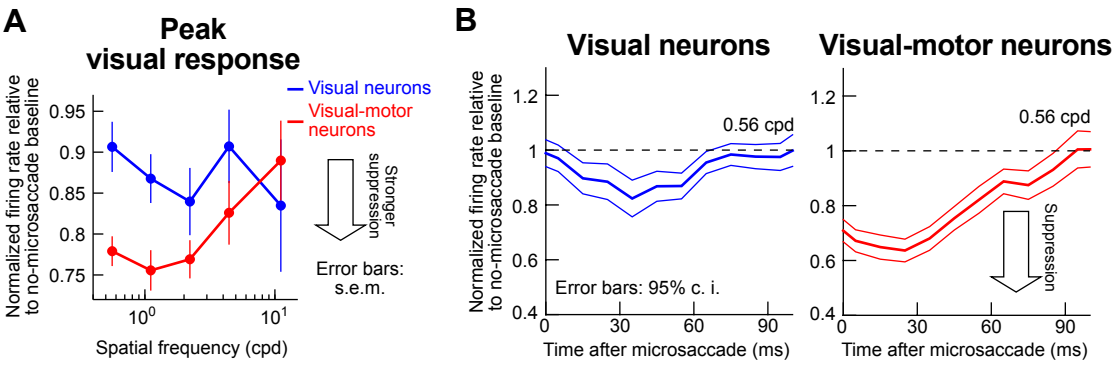
A
Peak
visual response
Visual neurons
Visual-motor
neurons
Normalized firing rate relative
to no-microsaccade baseline
0.95
0.9
0.85
0.8
0.75
10^0
10^1
Spatial frequency (cpd)
Stronger
suppression
Error bars:
s.e.m.
B
Visual neurons
Visual-motor neurons
0.56 cpd
0.56 cpd
1.2
1
0.8
0.6
0.4
Error bars: 95% c. i.
Suppression
0
30
60
90
Time after microsaccade (ms)
Time after microsaccade (ms)

A

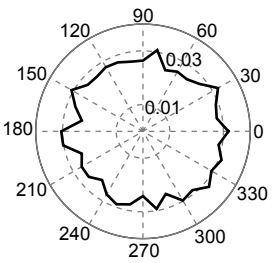
Microsaccade directions
relative to RF stimulus
90
60
30
0
330
300
270
240
210
180
150
120
0.03
0.01

B

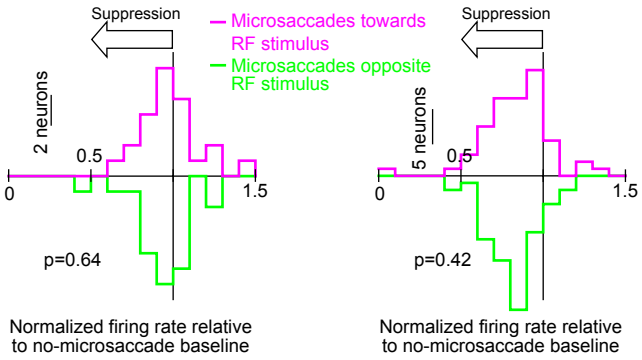
Visual neurons
(0.56 cpd)
Visual-motor neurons
(0.56 cpd)
Suppression
Microsaccades towards
RF stimulus
Microsaccades opposite
RF stimulus
2 neurons
5 neurons
0.5
0
1.5
p=0.64
p=0.42
Normalized firing rate relative
to no-microsaccade baseline
Normalized firing rate relative
to no-microsaccade baseline

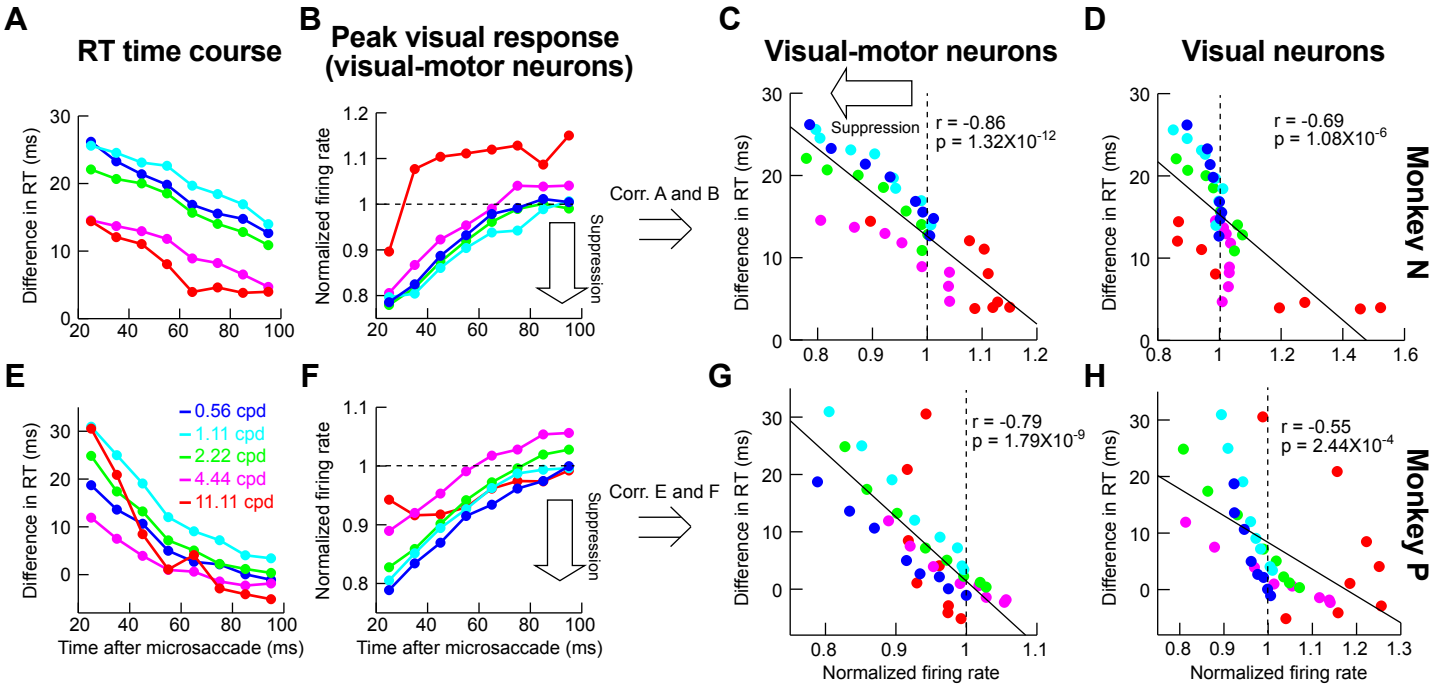
A
RT time course
B
Peak visual response
(visual-motor neurons)
C
Visual-motor neurons
D
Visual neurons
Difference in RT (ms)
Normalized firing rate
Suppression
Corr. A and B
r = -0.86
p = 1.32X10-12
r = -0.69
p = 1.08X10-6
Monkey N
E
F
G
H
0.56 cpd
1.11 cpd
2.22 cpd
4.44 cpd
11.11 cpd
Time after microsaccade (ms)
Corr. E and F
r = -0.79
p = 1.79X10-9
r = -0.55
p = 2.44X10-4
Monkey P

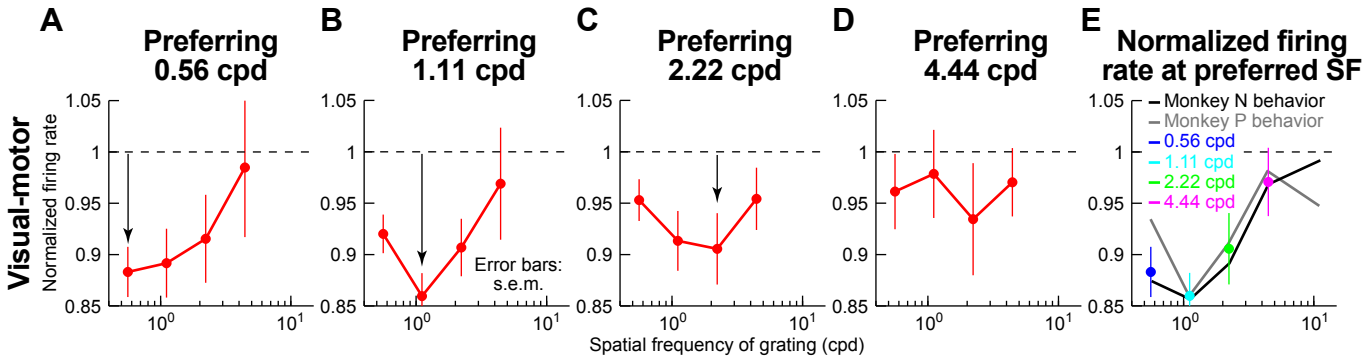
A
Preferring 0.56 cpd
B
Preferring 1.11 cpd
C
Preferring 2.22 cpd
D
Preferring 4.44 cpd
E
Normalized firing rate at preferred SF
Visual-motor
Normalized firing rate
1.05
1
0.95
0.9
0.85
10^0
10^1
Error bars: s.e.m.
Spatial frequency of grating (cpd)
Monkey N behavior
Monkey P behavior
0.56 cpd
1.11 cpd
2.22 cpd
4.44 cpd

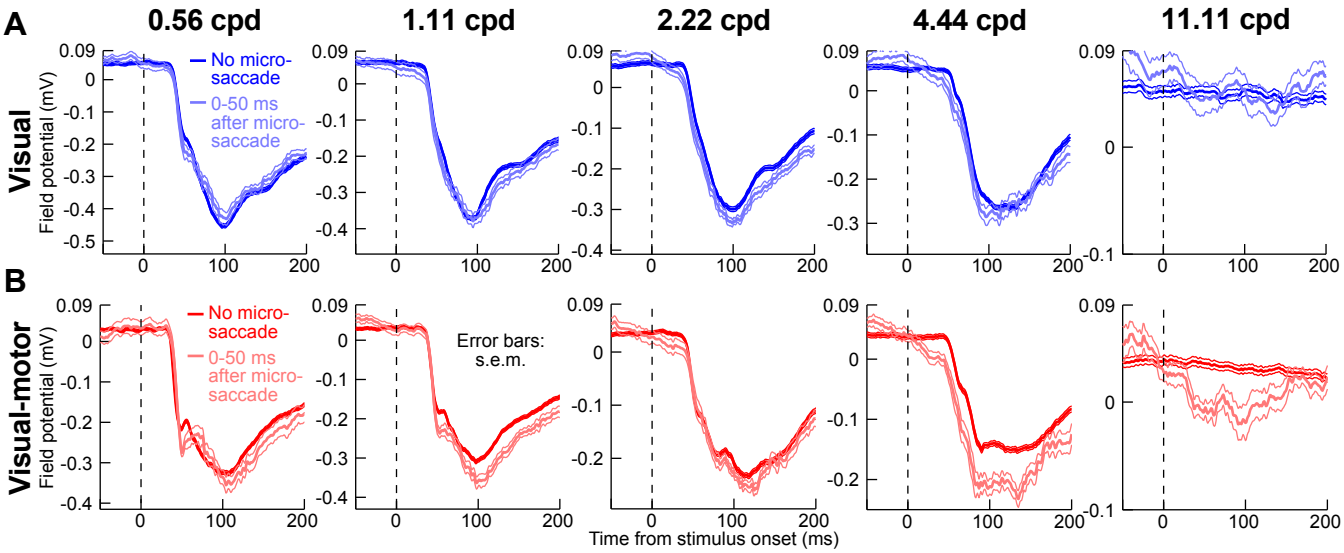
A
0.56 cpd
1.11 cpd
2.22 cpd
4.44 cpd
11.11 cpd
Visual
Field potential (mV)
No micro-saccade
0-50 ms after micro-saccade
B
Visual-motor
Field potential (mV)
No micro-saccade
0-50 ms after micro-saccade
Error bars: s.e.m.
Time from stimulus onset (ms)

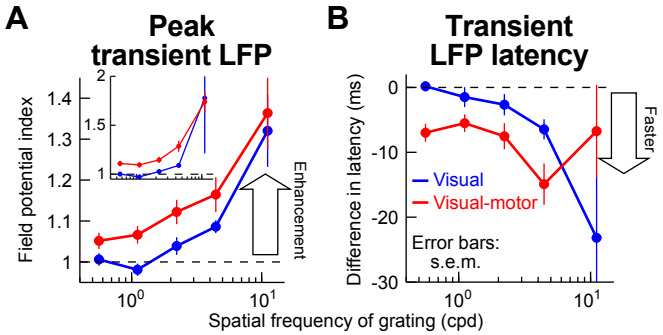
A
Peak transient LFP
Field potential index
1.4
1.3
1.2
1.1
1
2
1.5
1
Enhancement
10^0
10^1
B
Transient LFP latency
Difference in latency (ms)
0
-10
-20
-30
Faster
Visual
Visual-motor
Error bars: s.e.m.
10^0
10^1
Spatial frequency of grating (cpd)

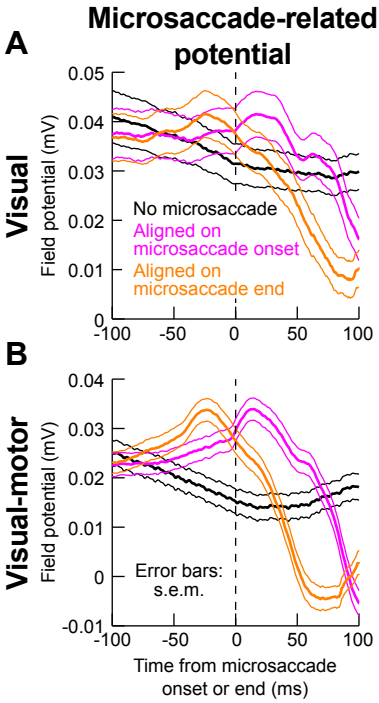
A
Microsaccade-related potential
Visual
Field potential (mV)
0.05
0.04
0.03
0.02
0.01
0
No microsaccade
Aligned on microsaccade onset
Aligned on microsaccade end
-100
-50
0
50
100
B
Visual-motor
Field potential (mV)
0.04
0.03
0.02
0.01
0
-0.01
Error bars: s.e.m.
-100
-50
0
50
100
Time from microsaccade onset or end (ms)

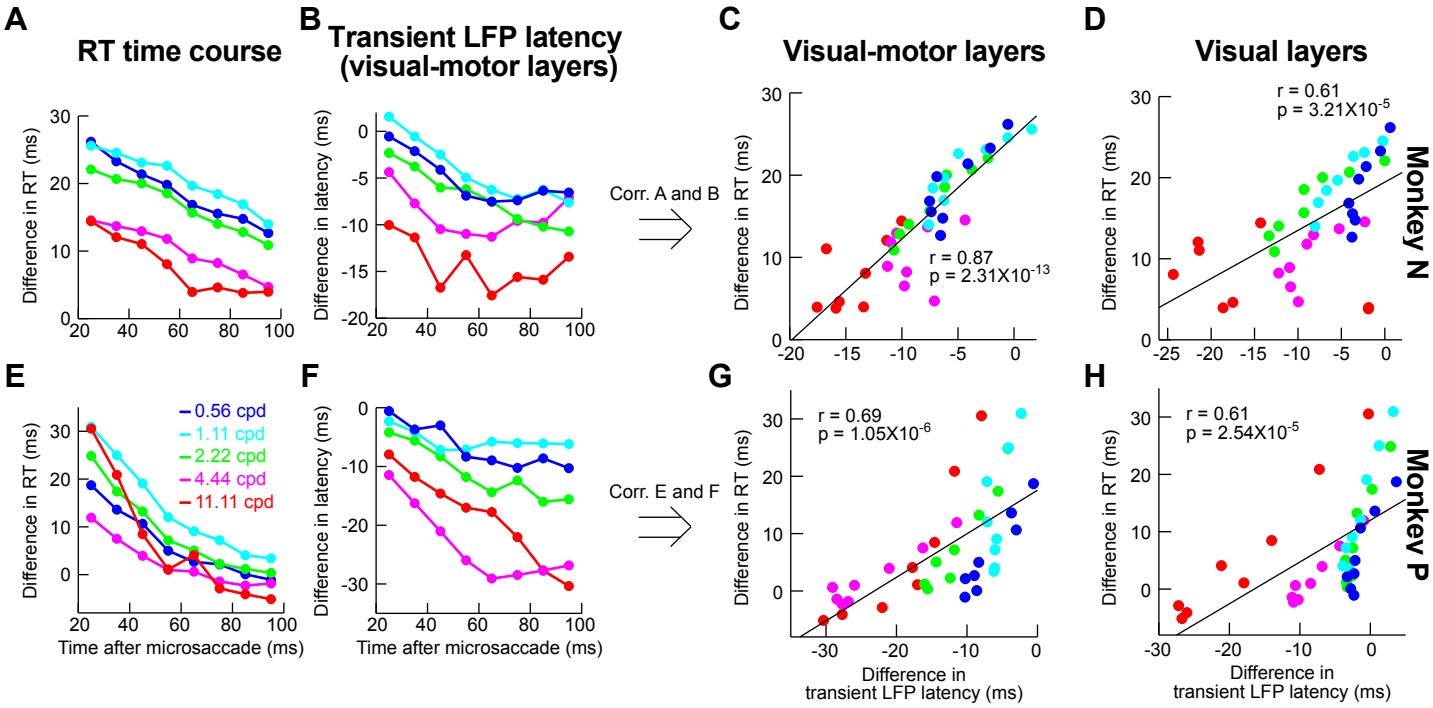
A
RT time course
B
Transient LFP latency
(visual-motor layers)
C
Visual-motor layers
D
Visual layers
Difference in RT (ms)
Difference in latency (ms)
Corr. A and B
r = 0.87
p = 2.31X10-13
r = 0.61
p = 3.21X10-5
Monkey N
E
F
G
H
0.56 cpd
1.11 cpd
2.22 cpd
4.44 cpd
11.11 cpd
Time after microsaccade (ms)
Corr. E and F
r = 0.69
p = 1.05X10-6
r = 0.61
p = 2.54X10-5
Monkey P
Difference in
transient LFP latency (ms)